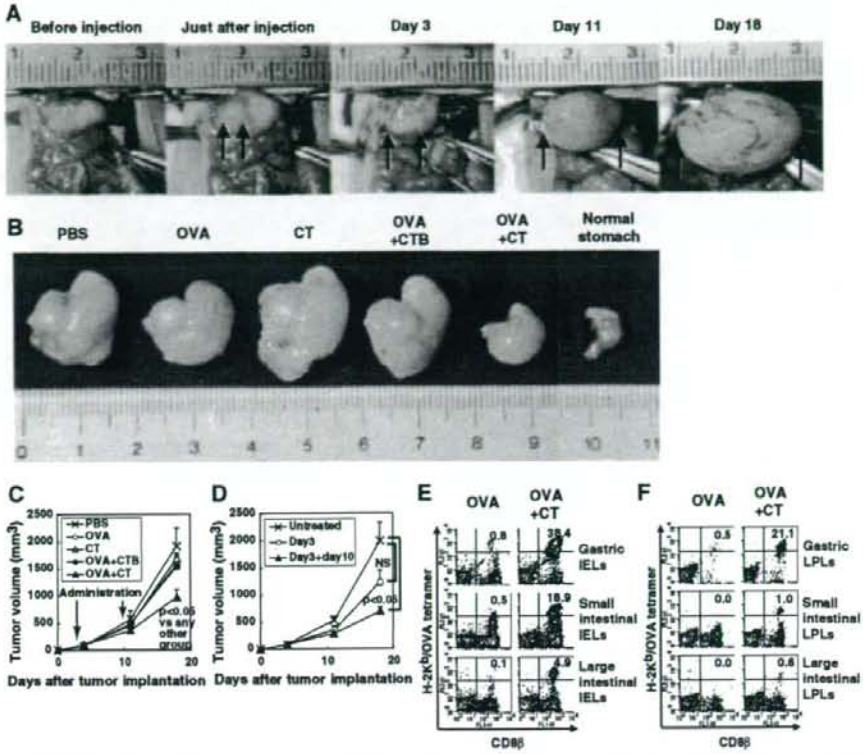

FIGURE 4. Suppression of the growth of a tumor implanted into gastric tissue by oral administration of OVA plus CT. *A*, Growth of visible tumor after implantation of E.G7-OVA cells into gastric tissue. C57BL/6 mice were implanted with 5×10^6 E.G7-OVA cells into the muscle layer of the stomach. Each day, the same mice were anesthetized and underwent an abdominal operation, and tumors were observed. Arrows point to both ends of the longer axis in the tumor. *B*, C57BL/6 mice were implanted with 5×10^6 E.G7-OVA cells into the muscle layer of the stomach. Three days later, tumor-bearing mice were orally administered PBS, OVA, CT, OVA plus CTB subunit, or OVA plus CT. Seven days later, the second oral administration was performed in the same manner. Stomachs were excised from the mice 18 days after tumor implantation, as well as from untreated, normal mice. *C*, Tumor volumes were calculated based on the formula described in *Materials and Methods*, and the results are shown as the mean ± SEM. The results were obtained from 9–13 mice per group. $p < 0.05$ indicates statistically significant difference between OVA plus CT (▲) and any other groups. *D*, C57BL/6 mice were implanted with E.G7-OVA cells in the stomach. Three days later, tumor-bearing mice were orally administered OVA plus CT or left untreated. Seven days later, some orally immunized mice were boosted in the same manner or left untreated. The results are shown as the mean ± SEM of 5–7 mice per group. $p < 0.05$ and NS indicate statistically significant and not significant differences, respectively, between the boosted (▲) and nonboosted (○) groups and the untreated group (×). *E* and *F*, Induction of CD8β and H-2K^b/OVA tetramer-positive cells in IELs (*E*) and LPLs (*F*) of the stomach, small intestine, or large intestine after oral administration of OVA plus CT. C57BL/6 mice were orally administered OVA or OVA plus CT once weekly for 2 wk. IELs and LPLs were collected from mice 3 days after the second oral administration. Cells were stained with PE-labeled H-2K^b/OVA tetramer and FITC-labeled anti-mouse CD8β. Each value represents the percentage of cells expressing both indicated markers. The results are representative of three independent experiments.

α-IEL chain)-positive cells in the collected samples were examined by flow cytometry. CD103 is highly expressed on >90% of IELs (29, 30) but on only 15% of SCs (31). In the present study, CD103-positive cells occupied >90% of IELs and ~15% of SCs (data not shown). Although a small number of OVA-specific TCR-expressing cells were detected in both IELs (4.5–5.0%) and SCs (1.0–1.5%) after oral administration of OVA plus CT in comparison with control H-2K^b/PB1-positive cells, H-2K^b/OVA tetramer-positive cells were not observed in mice treated with OVA alone (Fig. 1*A*). Such OVA peptide-specific TCR-expressing cells were TCRγδ negative (data not shown) and both CD8α and β positive (Fig. 1*B*). The number of tetramer-positive cells, to which the magnitude of direct OVA-specific cytotoxicity closely corresponded, was maximal at day 7 after oral immunization with both IELs and SCs (Fig. 1*B*), but it did not correspond to NK cell activity as measured against YAC-1 targets (Fig. 1*C*). The results clearly demonstrate that direct OVA-specific CTL cytotoxicity is dominantly observed in mucosal IELs after primary oral administration of OVA plus CT.

Augmentation and kinetics of direct OVA-specific cytotoxicity by CD8αβ CTLs among IELs and SCs via oral boosting with OVA plus CT at day 7 after the primary administration

As shown above, because only 4.5–5.0% of IELs were temporarily activated by a one-shot oral administration, we extensively examined the effect of oral boosting with OVA plus CT at various days after primary immunization. The number of H-2K^b/OVA tetramer-positive cells was significantly enhanced among IELs but not among SCs when primed mice were boosted (Fig. 2*A*). Such an effect was highest when mice were boosted at day 7 after initial

priming (data not shown). Tetramer-positive cells were again TCRβ-, CD8α-, and CD8β-positive IELs and their number peaked at day 3 after boosting (Fig. 2*B*). Correspondingly, direct OVA-specific cytotoxicity was greatly enhanced among IELs and the maximal cytotoxicity of IELs was observed at day 3 after boosting (Fig. 2*C*), although such direct cytotoxicity appeared to be completely lost in SCs (Fig. 2*C*). Nonetheless, SCs showed good epitope-specific cytotoxicity similar to that of IELs when they were restimulated in vitro with irradiated E.G7-OVA (Fig. 2*D*), suggesting that the priming effect by the oral administration of OVA plus CT also remained in systemic SCs.

It should be noted that the memory of OVA-specific CTLs persisted among IELs but not SCs. When secondary boosting with OVA plus CT was performed even 6 mo after primary boosting at day 7, the number of H-2K^b/OVA tetramer-positive cells was still detected at ~6% in IELs, and they showed remarkable direct cytotoxicity of ~84.5% against E.G7-OVA cells and 58.4% against EL4 cells pulsed with OVA peptide 3 days after secondary boosting (data not shown). Again, we could not detect any measurable direct cytotoxicity in the SCs of secondary boosted mice (data not shown).

Both CTA and CTB subunits are required to induce direct OVA-specific cytotoxicity in IELs

CT is comprised of a single A subunit, CTA, and five B subunits, CTB. When OVA was administered orally to mice with either 10 μg of CTA or an equal amount of CTB, H-2K^b/OVA tetramer-positive cells as well as direct OVA-specific cytotoxicity could not be detected in IELs (Fig. 3, *A* and *B*) and SCs (data not shown), although a significant number of tetramer-positive cells and strong direct OVA-specific cytotoxicity were observed among IELs of mice administered orally with OVA plus 10 μg of intact CT (Fig. 3, *A* and *B*). Even when using 50 μg of CTA or CTB for the administration of OVA, direct cytotoxicity was not observed (data not shown); therefore, both CTA and CTB subunits are required to induce direct Ag-specific cytotoxicity.

Effects of oral administration and booting with OVA plus CT on OVA-expressing tumor growth established in the stomach

We then examined in vivo antitumor effects of oral administration with tumor Ag plus CT on already established tumors growing in mice. C57BL/6 mice were implanted with 5×10^6 syngeneic E.G7-OVA cells into the muscle layer of the stomach (Fig. 4*A*). Three days later, tumor-bearing mice (Fig. 4*A*) were orally administered various combinations of OVA plus adjuvant and boosted with the same materials 7 days after the initial oral administration. To our surprise, tumor growth in the stomach of mice orally administered OVA plus CT twice was visually (Fig. 4*B*) and significantly ($p < 0.05$; Fig. 4*C*) suppressed on day 18 after tumor implantation as compared with other control groups such as OVA plus CTB or CT alone. However, when tumor-bearing mice were orally administered OVA plus CT once and without boosting, no statistically significant suppression was observed on day 18 as compared with untreated control mice, although a slight suppressive effect could be seen (Fig. 4*D*). Therefore, two oral administrations of tumor-Ag plus CT with an appropriate interval induced significant ongoing tumor suppression.

As previously shown, direct OVA-specific cytotoxicity among small intestinal IELs was greatly enhanced after boosting with OVA plus CT (Fig. 2, *A*, *B*, and *C*). We also examined whether direct OVA-specific CTLs were induced in the IELs and LPLs of the stomach, small intestine, and large intestine from boosted mice in which gastric tumor growth was significantly suppressed. We observed an increase in the number of H-2K^b/OVA tetramer-positive

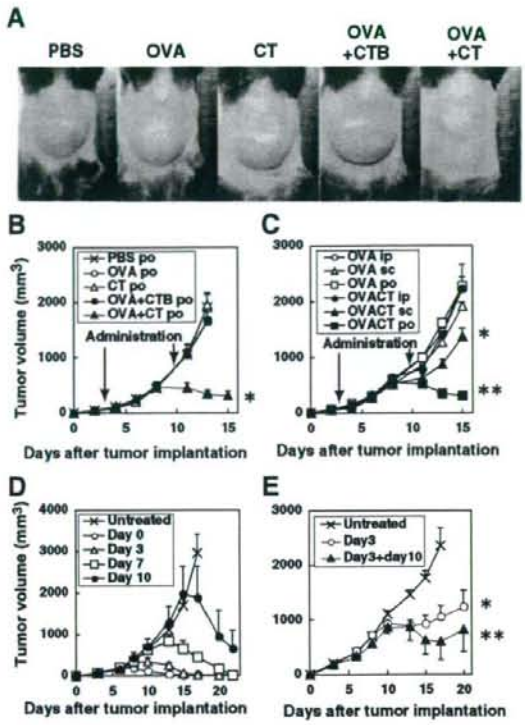

FIGURE 5. Suppression of intradermal tumor growth by oral administration with OVA plus CT. C57BL/6 mice were implanted intradermally with 5×10^6 E.G7-OVA cells. Three days later, tumor-bearing mice were orally administered PBS, OVA, CT, OVA plus CTB subunit, or OVA plus CT. Seven days later, the second oral administration was performed in the same manner. *A*, Visual suppressive effect of oral inoculation of OVA plus CT on dermal tumor growth. *B*, Tumor volumes were calculated based on the formula described in *Materials and Methods* and the results are shown as the mean ± SEM. Results were obtained from 5–6 mice per group. The asterisk (*) indicates statistically significant difference between the OVA plus CT group (closed triangle) and any other group at 11 days ($p < 0.05$) and 13 days ($p < 0.005$) after tumor inoculation. *C*, C57BL/6 mice were implanted intradermally with E.G7-OVA cells. Three days later, tumor-bearing mice were intraperitoneally (ip), subcutaneously (sc), or orally (po) administered OVA alone or OVA plus CT. Seven days later, the second treatment was performed in the same manner. The results are shown as the mean of tumor volumes ± SEM. Results were obtained from 5–6 mice per group. The asterisk (*) shows statistically significant differences ($p < 0.05$) between the s.c. OVA plus CT group (▲) and the s.c. OVA alone group at days 11, 13, and 15 after tumor implantation, and the two asterisks (**) indicate significant differences ($p < 0.01$) between the oral OVA plus CT group (■) and the oral OVA alone group on the same days. *D*, C57BL/6 mice were implanted intradermally with E.G7-OVA cells. The mice were orally administered once with OVA plus CT at day 0, 3, 7, or 10 after tumor implantation. The results are shown as the mean of tumor volumes ± SEM. Results were obtained from 10–12 mice per group. In single orally administered groups, significant tumor regression ($p < 0.05$) was observed at 7 days after oral administration compared with the untreated group. *E*, C57BL/6 mice were implanted intradermally with E.G7-OVA cells. Three days later, tumor-bearing mice were orally administered a low dose (10 mg) of OVA plus CT. Seven days later, some orally administered mice were boosted in the same manner. The results obtained from 5- mice per group are shown as the mean of tumor volumes ± SEM. The asterisk (*) indicates statistically significant differences ($p < 0.01$) between the nonboosted (○) and untreated mice (×) groups at days 15 and 17 after tumor implantation, and the two asterisks (**) indicate significant differences ($p < 0.005$) between the boosted (▲) and untreated groups on the same days.

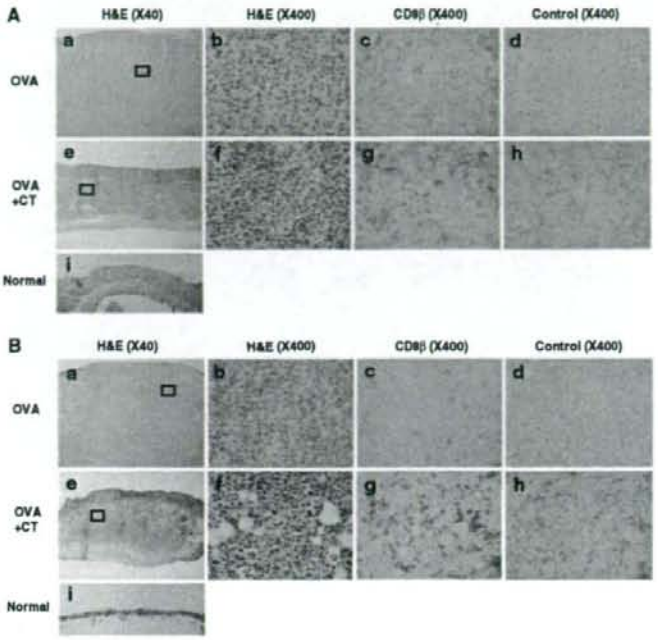

FIGURE 6. Infiltration of CD8$\alpha\beta$ positive lymphocytes into tumor tissues in mice orally administered OVA plus CT. C57BL/6 mice were implanted with 5×10^6 E.G7-OVA cells into the muscle layer of the stomach (*A*, *a–h*) or skin (*B*, *a–h*). Three days later, tumor-bearing mice were orally administered OVA (*A*, *a–d*, and *B*, *a–d*) or OVA plus CT (*A*, *e–h* and *B*, *e–h*). Seven days later, the second oral administration was performed in the same manner. Gastric and dermal tumor tissues were removed from mice 3 days after the second oral boost. Frozen sections of tumor tissues and normal tissues were prepared and stained with H&E (*A*, *a*, *b*, *e*, *f*, and *i* and *B*, *a*, *b*, *e*, *f*, and *i*) or immunohistochemically stained with biotin-conjugated rat anti-CD8β mAb (*A*, *c* and *g*, and *B*, *c* and *g*) or control isotype-matched rat IgG2a Ab (*A*, *d* and *h*, and *B*, *d* and *h*). Image magnification is either ×40 (*A*, *a*, *e*, and *i* and *B*, *a*, *e*, and *i*) or ×400 (*A*, *b–d* and *f–h* and *B*, *b–d* and *f–h*). *A*, *b* and *f* and *B*, *b* and *f* are enlarged images (×400) of the squared areas in the images (×40) of *A*, *a* and *e* and *B*, *a* and *e*, respectively.

cells among IELs in the stomach (38.4%) as well as the small (18.9%) and large intestine (4.9%) of tumor-suppressed mice (Fig. 4*E*) and also among LPLs in the stomach (21.1%) as well as the small (1.0%) and large (0.6%) intestine (Fig. 4*F*). Thus, the ability of LPLs to suppress tumor growth may be weaker than that of IELs. The results suggest that oral administration of Ag plus intact CT with appropriate mucosal boosting apparently suppressed the already established tumor growth in gastric tissue, particularly after oral boosting, probably through the activation of Ag-specific CTLs in the mucosal compartment.

Effects of oral administration and boosting with OVA plus CT on already established OVA-expressing dermal tumor growth

Next, we investigated the effect of the oral administration of tumor Ag plus CT on tumor growth in the skin, where the digestive tract is not directly associated. Mice were implanted with 5×10^6 E.G7-OVA cells intradermally. Three days later, tumor-bearing mice were orally administered various combinations of OVA plus adjuvant and boosted with the same materials 7 days after the initial oral administration. Interestingly, intradermal tumor growth was again strongly suppressed visually 11 days after tumor implantation in the dermis of mice orally administered OVA plus CT as compared with various other groups (Fig. 5*A*). This visual effect was confirmed by calculating the volume of the tumors established at day 11 and day 13 in each group ($p < 0.05$ and $p < 0.005$, respectively; Fig. 5*B*). We also examined the effect of the administration of tumor Ag plus CT via various routes on intradermal tumor growth. Although a slight suppression was observed by s.c. inoculation of OVA plus CT, tumor growth was not suppressed at all by i.p. administration in comparison with the oral treatment group (Fig. 5*C*). It should be noted that tumor growth in the dermis was markedly suppressed even by a single oral administration of OVA plus CT on day 0, 3, 7, or 10 after tumor implantation (Fig. 5*D*). In each group, tumor growth was suppressed ($p < 0.05$) and the tumor volume was small around 7 days after oral administration. Unexpectedly, there was almost no difference in the suppressive effects on tumor growth between mice treated with a single administration and boosted mice showing much stronger direct cytotoxicity (data not shown). However, when the dosage quantity of OVA was decreased by one-tenth, tumor growth in boosted mice was more significantly ($p < 0.005$) suppressed than in nonboosted mice ($p < 0.01$; Fig. 5*E*). Collectively, the results indicate that the oral administration of tumor Ag plus CT with appropriate mucosal boosting may induce a remarkable suppression of already established tumor growth in the skin via mucosally generated CTLs.

Infiltration of CD8$\alpha\beta$-positive cells in suppressed tumor tissues

We thus examined whether OVA-specific CD8$\alpha\beta$-positive CTLs were actually seen in suppressed tumor tissues such as the stomach and dermis. To determine tumor-infiltrating CD8$\alpha\beta^+$ cells, immunohistochemical staining was performed using biotin-conjugated rat anti-CD8β Ab (Fig. 6*A*, *c* and *g* and *B*, *c* and *g*) or control isotype-matched rat IgG2a Ab (Fig. 6*A*, *d* and *h* and *B*, *d* and *h*). Indeed, although mononuclear cells were seen in the gastric tumor tissues of mice treated with OVA alone, CD8$\alpha\beta$-positive cells were not observed at all (Fig. 6*A*, *a–d*). In contrast, infiltration of inflammatory mononuclear cells together with CD8$\alpha\beta$-positive cells was observed in suppressed gastric tumor tissues (Fig. 6*Ag*). As shown in Fig. 6*Ai*, normal gastric tissue is composed of the epithelium, lamina propria, lamina muscularis mucosae, muscle layer, and serosa from the inside surface in sequence. As compared with normal gastric tissue, a great number of large tumor cells (EG.7-OVA) were mainly found between the lamina muscularis mucosae and serosa of tumor-implanted tissues (Fig. 6*A*, *a* and *b*) and the infiltration of tumor cells into the lamina propria over the lamina muscularis mucosae was also observed (data not shown). However, in suppressed gastric tumor tissues (Fig. 6*Ae*) the tumor cell layer under the lamina muscularis mucosae was markedly thinner than that of an unsuppressed tumor (Fig. 6*Aa*), in which

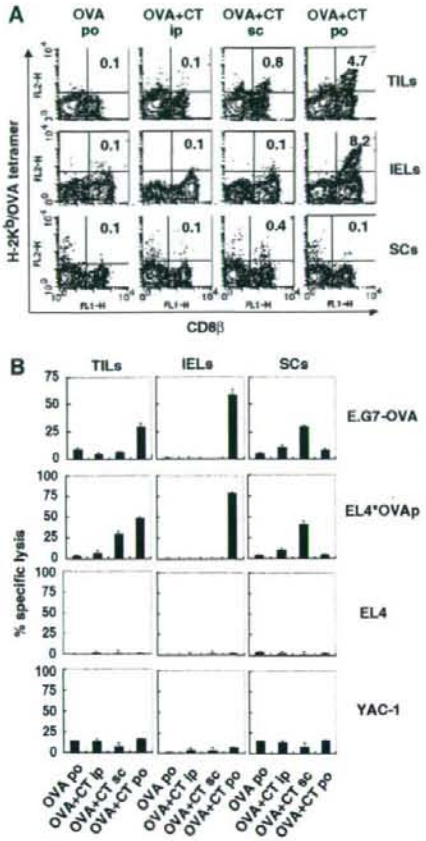

FIGURE 7. Detection of OVA-specific CTLs in TILs. C57BL/6 mice were implanted intradermally with E.G7-OVA cells. Three days later, mice were orally (po), subcutaneously (sc), or intraperitoneally (ip) administered OVA plus CT or orally treated with OVA. Seven days later, the second oral administration was performed in the same manner. TILs, IELs, and SCs were collected from mice 3 days after the second oral administration. *A*, TILs, IELs and SCs were double stained with PE-labeled H-2K^b/OVA tetramer and FITC-labeled anti-mouse CD8β. *B*, OVA-specific CTL responses of TILs, IELs, and SCs were measured by a ^{51}Cr-release assay using E.G7-OVA cells, YAC-1 cells, and EL4 cells pulsed with or without OVA peptide as targets. The E:T ratio is 5:1 in TILs, or 100:1 in IELs and SCs. The results are shown as the mean ± SD in triplicate of pooled cells from three mice. The results are representative of three independent experiments.

tumor cells almost never infiltrated the lamina propria over the lamina muscularis mucosae. Similarly, as for dermal tumor tissues, mononuclear cells together with CD8$\alpha\beta$-positive cells were not observed in mice treated with OVA alone (Fig. 6*B*, *a–d*), whereas the infiltration of a large number of mononuclear cells and CD8$\alpha\beta$-positive cells was observed in suppressed dermal tumor tissues (Fig. 6*B*, *e–g*). Dermal tumor sections were not stained with control isotype-matched rat IgG (Fig. 6*B*, *d* and *h*). As shown in Fig. 6*Bi*, normal skin is composed of epidermides and dermis from the surface in sequence. In tumor cell-implanted dermal tissues, although the infiltration of mononuclear cells or CD8$\alpha\beta$-positive cells was not observed, many large tumor cells were found thickly beneath the epidermides (Fig. 6*B*, *a* and *b*); however, when tumor cell-implanted mice were treated with OVA plus CT, most tumor cells became necrotic or apoptotic (Fig. 6*B*, *e* and *f*).

Measurement of tumor-specific cytotoxic activity by tumor-infiltrating cells in tumor-suppressed mice

To confirm whether infiltrated CD8$\alpha\beta$-positive T cells achieved OVA-specific cytotoxicity, we isolated TILs containing both mononuclear cells and CD8$\alpha\beta$-positive T cells from suppressed dermal tumor tissues as well as from their IELs and SCs. As expected, the number of H-2K^b/OVA tetramer-positive cells increased in both the TILs and IELs but not in the SCs of mice bearing suppressed tumors induced by oral administration with OVA plus CT as compared with mice inoculated with OVA plus CT via another route (Fig. 7*A*), and those increased tetramer-positive cells showed significant direct OVA-specific CTL activity (Fig. 7*B*). It should be noted that, although the number of increased cells specific for the H-2K^b/OVA tetramer was small in mice inoculated with OVA plus CT s.c., both the TILs (0.8%) and the SCs (0.4%) but not the IELs (0.1%) of the mice represented a detectable level of direct OVA-specific cytotoxicity (Fig. 7*B*). These findings suggest that s.c. immunization with Ag plus CT may preferably activate systemic (splenic) Ag-specific CTLs rather than local (intraepithelial) CTLs. Moreover, NK cell cytotoxicity determined against YAC-1 cells was not observed in TILs, IELs, and SCs by oral, s.c., or i.p. immunization of OVA plus CT (Fig. 7*B*), indicating that the suppression of tumor growth was mainly mediated by CD8$\alpha\beta$ CTLs rather than by NK cell cytotoxicity.

Discussion

In the present study we demonstrated that when OVA plus intact CT was orally administered into mice, direct OVA-specific cytotoxicity was dominantly induced in IELs rather than SCs after the first oral priming, and direct OVA-specific cytotoxicity was remarkably expanded in IELs but not in SCs after oral boosting with the same doses of OVA plus CT. Such OVA-specific CTLs were thymic conventional K^b class I MHC molecule-restricted TCR$\alpha\beta^+$ CD8$\alpha\beta$ T cells (32). Moreover, the growth of the OVA-expressing tumor E.G7-OVA thymoma, established previously either in the stomach or dermis, was significantly suppressed by the oral administration of OVA plus CT. Furthermore, marked infiltration of OVA-specific TCR$\alpha\beta^+$ CD8$\alpha\beta$ CTLs with direct cytotoxicity in reduced tumor tissues was observed. These results suggest that activated CTLs with specific cytotoxicity generated at mucosal compartments by oral administration with OVA plus intact CT may be responsible for already established tumor regression.

The majority of tumor regression studies associated with activation of the immune system have focused on systemic immunity observed in the spleen, lymph nodes, and circulating blood rather than local mucosal immunity seen in gut IELs. Those studies have demonstrated only preventative results for tumor establishment by preadministration of tumor Ag plus a suitable adjuvant. In addition, to our knowledge only one study has been shown to suppress already established tumor growth by activating and expanding tumor infiltrating CD8$^+$ CTLs (23). In that study, i.v. vaccination with DCs prepulsed ex vivo with OVA-CT at day 3 and boosted at day 10 after OVA-expressing E.G7 tumor injection induced complete rejection of a visible tumor within 3 wk after the first treatment. Although the inoculation route and the materials for vaccination were different from ours, the timing of the priming and boosting to induce the suppression of already established tumor growth correlated exactly, suggesting that their methods may also initiate strong mucosal direct cytotoxicity mediated through CD8$^+$ CTLs.

Similar to our findings, they also showed that immunization with OVA-CT but not with CTB-conjugated OVA (OVA-CTB)-prepulsed DCs could successfully induce complete rejection of already established tumor growth, although OVA-CTB-prepulsed DC inoculation prevented tumor establishment but not ongoing tumor growth in the skin. Moreover, they insisted that OVA has to be coupled to CT and should be loaded onto DCs for therapeutic DC vaccination based on the observation that neither OVA-CT nor DCs pulsed with unconjugated OVA plus CT could prevent tumor progression. Nonetheless, our findings shown here apparently indicate that we were able to induce effective suppression of ongoing tumor growth by simple oral administration with unconjugated OVA and CT. These results suggest that we may control already established tumor growth at the surface compartments by activating mucosal $CD8^+$ CTLs via orally administered tumor Ag with a suitable mucosal adjuvant. Also, when OVA-CT is orally administered, the conjugation between OVA and CT may be broken through digestion by enzymes secreted in the gastrointestinal tract. Recently, we have reported that modification of OVA in the gastrointestinal tract is essential for oral tolerance induction against OVA (33). Therefore, it is possible that gastrointestinal digestion or modification of OVA may facilitate the delivery of OVA Ag into DCs, critical APCs for OVA-specific CTL induction.

For the efficient induction of such OVA-specific CTLs in vivo using DCs, Eriksson et al. have reported that OVA-CT-prepulsed DC immunization required at least two DC injections, reflecting the priming/boosting procedure (23); however, we have observed that a single oral administration of OVA plus CT seems sufficient to induce effective CTLs to prevent E.G7-OVA thymoma growth, particularly in the skin. This may be because mucosally activated CTLs through oral immunization may be more potent than systemically activated CTLs to suppress transplanted tumors at the mucosal compartment, and oral administration of OVA plus CT seems more efficient to induce mucosal CTLs than i.v. Ag-loaded DC inoculation. Further studies will be needed to explain the differences.

Although both CT-conjugated-OVA and CTB-conjugated OVA are cross-presented by MHC class I in DCs, only CT-OVA but not CTB-OVA cross-primes OVA-specific $CD8^+$ CTLs in vivo (23, 34). Additionally, DCs pulsed with intact OVA alone cannot cross-present and cross-prime CTLs (23). For the cross-priming of Ag-specific CTLs by Ag-captured immature DCs, maturation signaling via some surface molecules such as TLR-3 in those DCs is essential (35, 36). Although whole CT up-regulates the expression of MHC class II, B7.1, and B7.2 molecules on DCs in vitro, neither CTA nor CTB alone up-regulates the levels of surface markers on DCs (37, 38). Also, the binding of CTB to GM1 on DCs seems necessary to efficiently take up both CT itself and Ag and to induce cross-presentation by MHC class I molecules on DCs, whereas CTA may not be taken up to affect DCs. When DCs from GM1-lacking mice were matured in vitro, CT failed to up-regulate the expression of maturation markers and, thus, the binding of B subunits in CT to GM1 molecules on DCs is essential for the induction of DC maturation (37). It has been reported that CTA is required to not only assist in maturation but also to generate the migration of DCs (39, 40); therefore, CTB-mediated matured DCs can initiate their migration to secondary lymphoid organs and colocalization with naive T cells (38). Indeed, CT-loaded but not CTB-loaded DCs could migrate from marginal zones to T cell zones in the spleen (39) and from the subepithelial dome region to T cell zones in PPs (40); therefore, both CTA and CTB were essential for cross-priming CTLs in vivo and neither CTA nor CTB alone could induce CTLs at various compartments (Fig. 3). Taken together, although the detailed mechanisms of efficient Ag presentation via MHC class I and the maturation and migration of DCs by CT are still unknown, digested OVA might be efficiently captured by immature gut mucosal DCs in the presence of CTB and the captured Ag may be cross-presented by MHC class I during DC maturation and migration in the presence of CTA, resulting in the induction of mucosal class I MHC molecule-restricted CTLs that may cause the regression of previously established tumors.

OVA-specific $CD8^+$ CTLs were induced among not only the IELs but also the LPLs of the stomach, small intestine, and large intestine by oral administration of OVA plus CT, a higher percentage of OVA-specific CD8 CTLs was observed in the stomach, small intestine, and large intestine in order, and more specific CTLs were always detected among IELs than among LPLs (Fig. 4, *E* and *F*). Thus, CTLs are much easier to be induced in the upper and more superficial portions of the gastrointestinal tract when Ags are orally administrated with intact CT.

It has been reported that DCs in gastric mucosa are increased in *Helicobacter pylori* (*Hp*)-infected mice and that the response of DCs and T cells to *Hp* Ag is critical for *Hp*-induced gastritis (41). In the present study, Ag-specific CTLs in the stomach might be generated by mucosally activated DCs in the presence of CT and infiltrate-implanted gastric tumor tissues. It is possible that intestinally activated CTLs might migrate to the tumor-implanted stomach, which might also cause CTL infiltration. Actually, such effector CTLs usually express high levels of $\alpha_4\beta_7$ integrin and can home in to the gastric (42), and small and large intestinal mucosa (43) where mucosal addressin cell-adhesion molecule-1 (MadCAM-1), the ligand of $\alpha_4\beta_7$ integrin, is constitutively expressed by post-capillary endothelial cells in small (44, 45) and large intestinal lamina propria (46). Moreover, the number of gastric $\alpha_4\beta_7^{high}$ T cells increased markedly by oral administration of CT in mice (42). It has also been reported that MAdCAM-1 expression is increased in the gastric mucosa after oral administration with cholera vaccine composed of CTB and formalin-inactivated *V. cholerae* (47); therefore, MadCAM-1-expression in gastric mucosa and the recruitment of effector $\alpha 4\beta 7^{high}$ T cells to gastric mucosa might be enhanced by oral administration of the CT adjuvant and, thus, OVA-specific effector CTLs might efficiently infiltrate the OVA Ag-expressing tumor region in the stomach.

In the present study, we found that the growth of dermally implanted tumors was also suppressed by the oral administration of tumor Ag plus whole intact CT. The actual mechanisms for such suppression remains to be elucidated, but there are at least three distinct possibilities: first, the migration of Ag-specific CTLs from the gastrointestinal tract to the skin; second, the migration of Ag-presenting DCs activated in the mucosal compartments by CT; and third, the migration of both cells from the gastrointestinal tract to the skin at the same time. It has been reported that the levels of CCR4 expression, which is associated with T cell homing to the skin, are increased in gastric T cells by infection with *Hp* in humans (48). Moreover, mucosal DCs that take up Ag might migrate to regional lymph nodes near the dermal tumor and prime the CTLs there, and the CTLs could effectively infiltrate dermal tumor tissue. Indeed, Belyakov et al. demonstrated an opposite mechanism in which skin-derived DCs containing heat-labile enterotoxin of *Escherichia coli* migrated to PPs and induced mucosal CTLs by transcutaneous immunization of an Ag and CT (49). Although the detailed mechanisms of this migration of DCs between skin and mucosa are unknown, they have clearly shown that DCs can migrate between the mucosa and skin. We are currently comparing the alteration of DCs in the mucosal compartment, spleen, and lymph nodes after oral administration of an Ag plus natural CT.

Unfortunately, such natural CT is not an appropriate mucosal adjuvant for human clinical investigation (50); however, studies

using natural CT would provide important and critical information about the effect of CT that would be useful for mucosal immune activation. Based on the findings obtained by using natural CT in a mouse model system, we could establish much safer protocols with a mutant CT (51) that induces adenosine diphosphate ribosylation and cyclic adenosine monophosphate formation, which may prevent severe diarrhea as well as retain adjuvant properties. Taken together, an artificial CT-based vaccine targeting DCs may provide a strategy for efficient CTL induction and avirulent mucosal cancer vaccination.

Our data also indicate that E.G7-OVA tumor growth was suppressed by OVA-specific CTLs but not NK cells (Fig. 7*B*). Vaccination with OVA-CT-pulsed DC protects against E.G7-OVA tumor development in vivo in wild-type, NK-depleted, and CD4-deficient mice but not in CD8-deficient mice (34), indicating that the E.G7-OVA tumor might be controlled by CD8 T cells but not by NK cells or CD4 T cells. In fact, TILs in the suppressed tumor did not show any NK-related cytotoxicity (Fig. 7*B*). Moreover, it has been demonstrated that in vitro pretreatment of NK cells with CT inhibits NK cell killing of tumor (YAC-1 or P815), because G proteins in NK cell membranes are ADP ribosylated with CT and ribosylation inhibits the lysis of tumor cells (52); therefore, NK cells do not seem to be involved in the suppression of E.G7-OVA growth in vivo.

It has been shown that activated CTLs but not naive CTLs can represent antitumor (22) or antivirus (12) responses in vivo. In the present study, already established E.G7 tumor growth can be suppressed only when OVA-specific CTLs that show specific cytotoxicity without requiring in vitro restimulation are induced, particularly in the mucosal compartment. To our knowledge, this is the first demonstration of the visual suppression of already established tumor growth by the simple oral administration of tumor Ag plus mucosal adjuvant. The findings shown in the present study herald a new era for cancer immunotherapy.

Acknowledgments

We thank Dr. Yoshihiro Kumagai and Yoshihiko Norose for useful discussions and advice.

Disclosures

The authors have no financial conflict of interest.

References

1. Franks, L. M., and M. A. Knowles. 2005. What is cancer? In *Introduction to the Cellular and Molecular Biology of Cancer*, 4th Ed. M. A. Knowles and P. J. Selby, eds. Oxford University Press, New York, pp. 1–24.
2. Finn, O. J. 2003. Cancer vaccines: between the idea and the reality. *Nat. Rev. Immunol.* 3: 630–641.
3. Czerkinsky, C., F. Anjuere, J. R. McGhee, A. George-Chandy, J. Holmgren, M. P. Kieny, K. Fujiyashi, J. F. Mestecky, V. Pierrefite-Carle, C. Rask, and J. B. Sun. 1999. Mucosal immunity and tolerance: relevance to vaccine development. *Immunol. Rev.* 170: 197–222.
4. Yuki, Y., and H. Kiyono. 2003. New generation of mucosal adjuvants for the induction of protective immunity. *Rev. Med. Virol.* 13: 293–310.
5. Takahashi, H. 2003. Antigen presentation in vaccine development. *Comp. Immunol. Microbiol. Infect. Dis.* 26: 309–328.
6. Hayday, A., E. Theodoridis, E. Ramsburg, and J. Shires. 2001. Intraepithelial lymphocytes: exploring the third way in immunology. *Nat. Immunol.* 2: 997–1003.
7. Offit, P. A., and K. I. Dudzik. 1989. Rotavirus-specific cytotoxic T lymphocytes appear at the intestinal mucosal surface after rotavirus infection. *J. Virol.* 63: 3507–3512.
8. Chardes, T., D. Buzoni-Gatel, A. Lepage, F. Bernard, and D. Bout. 1994. *Toxoplasma gondii* oral infection induces specific cytotoxic CD8 $\alpha\beta^+$ Thy-1$^+$ gut intraepithelial lymphocytes, lytic for parasite-infected enterocytes. *J. Immunol.* 153: 4596–4603.
9. Muller, S., M. Buhler-Jungo, and C. Mueller. 2000. Intestinal intraepithelial lymphocytes exert potent protective cytotoxic activity during an acute virus infection. *J. Immunol.* 164: 1986–1994.
10. Taunk, J., A. I. Roberts, and E. C. Ebert. 1992. Spontaneous cytotoxicity of human intraepithelial lymphocytes against epithelial cell tumors. *Gastroenterology* 102: 69–75.
11. Roberts, A. I., S. M. O'Connell, L. Biancone, R. E. Brolin, and E. C. Ebert. 1993. Spontaneous cytotoxicity of intestinal intraepithelial lymphocytes: clues to the mechanism. *Clin. Exp. Immunol.* 94: 527–532.
12. Kuribayashi, H., A. Wakabayashi, M. Shimizu, H. Kaneko, Y. Norose, Y. Nakagawa, J. Wang, Y. Kumagai, D. H. Margulies, and H. Takahashi. 2004. Resistance to viral infection by intraepithelial lymphocytes in HIV-1 P18-I10-specific T-cell receptor transgenic mice. *Biochem. Biophys. Res. Commun.* 316: 356–363.
13. Takahashi, H., J. Cohen, A. Hosmalin, K. B. Cease, R. Houghten, J. L. Cornette, C. DeLisi, B. Moss, R. N. Germain, and J. A. Berzofsky. 1988. An immunodominant epitope of the human immunodeficiency virus envelope glycoprotein gp160 recognized by class I major histocompatibility complex molecule-restricted murine cytotoxic T lymphocytes. *Proc. Natl. Acad. Sci. USA* 85: 3105–3109.
14. Williams, N. A., T. R. Hirst, and T. O. Nashar. 1999. Immune modulation by the cholera-like enterotoxins: from adjuvant to therapeutic. *Immunol. Today* 20: 95–101.
15. Lencer, W. I., and B. Tsai. 2003. The intracellular voyage of cholera toxin: going retro. *Trends Biochem. Sci.* 28: 639–645.
16. Elson, C. O., and W. Ealding. 1984. Generalized systemic and mucosal immunity in mice after mucosal stimulation with cholera toxin. *J. Immunol.* 132: 2736–2741.
17. Marinaro, M., H. F. Staats, T. Hiroi, R. J. Jackson, M. Coste, P. N. Boyaka, N. Okahashi, M. Yamamoto, H. Kiyono, H. Bluethmann, et al. 1995. Mucosal adjuvant effect of cholera toxin in mice results from induction of T helper 2 (Th2) cells and IL-4. *J. Immunol.* 155: 4621–4629.
18. Bowen, J. C., S. K. Nair, R. Reddy, and B. T. Rouse. 1994. Cholera toxin acts as a potent adjuvant for the induction of cytotoxic T-lymphocyte responses with non-replicating antigens. *Immunology* 81: 338–342.
19. Carbone, F. R., and M. J. Bevan. 1989. Induction of ovalbumin-specific cytotoxic T cells by in vivo peptide immunization. *J. Exp. Med.* 169: 603–612.
20. Moore, M. W., F. R. Carbone, and M. J. Bevan. 1988. Introduction of soluble protein into the class I pathway of antigen processing and presentation. *Cell* 54: 777–785.
21. Porgador, A., H. F. Staats, B. Faiola, E. Gilboa, and T. J. Palker. 1997. Intranasal immunization with CTL epitope peptides from HIV-1 or ovalbumin and the mucosal adjuvant cholera toxin induces peptide-specific CTLs and protection against tumor development in vivo. *J. Immunol.* 158: 834–841.
22. Dalyot-Herman, N., O. F. Bathe, and T. R. Malek. 2000. Reversal of CD8$^+$ T cell ignorance and induction of anti-tumor immunity by peptide-pulsed APC. *J. Immunol.* 165: 6731–6737.
23. Eriksson, K., J. B. Sun, I. Nordstrom, M. Fredriksson, M. Lindblad, B. L. Li, and J. Holmgren. 2004. Coupling of antigen to cholera toxin for dendritic cell vaccination promotes the induction of MHC class I-restricted cytotoxic T cells and the rejection of a cognate antigen-expressing model tumor. *Eur. J. Immunol.* 34: 1272–1281.
24. Taguchi, T., J. R. McGhee, R. L. Coffman, K. W. Beagley, J. H. Eldridge, K. Takatsu, and H. Kiyono. 1990. Analysis of Th1 and Th2 cells in murine gut-associated tissues: frequencies of CD4$^+$ and CD8$^+$ T cells that secrete IFN-γ and IL-5. *J. Immunol.* 145: 68–77.
25. Takahashi, M., E. Osono, Y. Nakagawa, J. Wang, J. A. Berzofsky, D. H. Margulies, and H. Takahashi. 2002. Rapid induction of apoptosis in CD8$^+$ HIV-1 envelope-specific murine CTLs by short exposure to antigenic peptide. *J. Immunol.* 169: 6588–6593.
26. Semple, J. W., and M. R. Szewczuk. 1986. Natural killer cells in murine muscular dystrophy: IV. Characterization of Percoll fractionated splenic and thymic natural killer cells and natural killer-sensitive thymocyte targets. *Clin. Immunol. Immunopathol.* 41: 116–129.
27. Belz, G. T., W. Xie, and P. C. Doherty. 2001. Diversity of epitope and cytokine profiles for primary and secondary influenza a virus-specific CD8$^+$ T cell responses. *J. Immunol.* 166: 4627–4633.
28. Nakatsuka, K., H. Sugiyama, Y. Nakagawa, and H. Takahashi. 1999. Purification of antigenic peptide from murine hepatoma cells recognized by class-I major histocompatibility complex molecule-restricted cytotoxic T-lymphocytes induced with B7-1-gene-transfected hepatoma cells. *J. Hepatol.* 30: 1119–1129.
29. Kilshaw, P. J., and K. C. Baker. 1988. A unique surface antigen on intraepithelial lymphocytes in the mouse. *Immunol. Lett.* 18: 149–154.
30. Russell, G. J., C. M. Parker, K. L. Cepek, D. A. Mandelbrot, A. Sood, E. Mizoguchi, E. C. Ebert, M. B. Brenner, and A. K. Bhan. 1994. Distinct structural and functional epitopes of the α E β 7 integrin. *Eur. J. Immunol.* 24: 2832–2841.
31. Lefrancois, L., T. A. Barrett, W. L. Havran, and L. Puddington. 1994. Developmental expression of the α IEL β 7 integrin on T cell receptor γ δ and T cell receptor α β T cells. *Eur. J. Immunol.* 24: 635–640.
32. Rocha, B., P. Vassalli, and D. Guy-Grand. 1994. Thymic and extrathymic origins of gut intraepithelial lymphocyte populations in mice. *J. Exp. Med.* 180: 681–686.
33. Wakabayashi, A., Y. Kumagai, E. Watari, M. Shimizu, M. Utsuyama, K. Hirokawa, and H. Takahashi. 2006. Importance of gastrointestinal ingestion and macromolecular antigens in the vein for oral tolerance induction. *Immunology* 119: 167–177.
34. Sun, J. B., K. Eriksson, B. L. Li, M. Lindblad, J. Azem, and J. Holmgren. 2004. Vaccination with dendritic cells pulsed in vitro with tumor antigen conjugated to cholera toxin efficiently induces specific tumoricidal CD8$^+$ cytotoxic lymphocytes dependent on cyclic AMP activation of dendritic cells. *Clin. Immunol.* 112: 35–44.

35. Fujimoto, C., Y. Nakagawa, K. Ohara, and H. Takahashi. 2004. Polyriboinosinic polyribocytidylic acid (poly(I:C))/TLR3 signaling allows class I processing of exogenous protein and induction of HIV-specific $CD8^+$ cytotoxic T lymphocytes. *Int. Immunol.* 16: 55–63.
36. Schulz, O., S. S. Diebold, M. Chen, T. I. Naslund, M. A. Nolte, L. Alexopoulou, Y. T. Azuma, R. A. Flavell, P. Liljestrom, and C. Reis e Sousa. 2005. Toll-like receptor 3 promotes cross-priming to virus-infected cells. *Nature* 433: 887–892.
37. Kawamura, Y. I., R. Kawashima, Y. Shirai, R. Kato, T. Hamabata, M. Yamamoto, K. Furukawa, K. Fujihashi, J. R. McGhee, H. Hayashi, and T. Dohi. 2003. Cholera toxin activates dendritic cells through dependence on GM1-ganglioside which is mediated by NF-κB translocation. *Eur. J. Immunol.* 33: 3205–3212.
38. Gagliardi, M. C., F. Sallusto, M. Marinaro, A. Langenkamp, A. Lanzavecchia, and M. T. De Magistris. 2000. Cholera toxin induces maturation of human dendritic cells and licences them for Th2 priming. *Eur. J. Immunol.* 30: 2394–2403.
39. Grdic, D., L. Ekman, K. Schon, K. Lindgren, J. Mattsson, K. E. Magnusson, P. Ricciardi-Castagnoli, and N. Lycke. 2005. Splenic marginal zone dendritic cells mediate the cholera toxin adjuvant effect: dependence on the ADP-ribosyltransferase activity of the holotoxin. *J. Immunol.* 175: 5192–5202.
40. Shreedhar, V. K., B. L. Kelsall, and M. R. Neutra. 2003. Cholera toxin induces migration of dendritic cells from the subepithelial dome region to T- and B-cell areas of Peyer's patches. *Infect. Immun.* 71: 504–509.
41. Drakes, M. L., S. J. Czinn, and T. G. Blanchard. 2006. Regulation of murine dendritic cell immune responses by *Helicobacter felis* antigen. *Infect. Immun.* 74: 4624–4633.
42. Michetti, M., C. P. Kelly, J. P. Kraehenbuhl, H. Bouzourene, and P. Michetti. 2000. Gastric mucosal $\alpha_4\beta_7$-integrin-positive CD4 T lymphocytes and immune protection against *Helicobacter* infection in mice. *Gastroenterology* 119: 109–118.
43. Lefrancois, L., C. M. Parker, S. Olson, W. Muller, N. Wagner, M. P. Schon, and L. Puddington. 1999. The role of β_7 integrins in CD8 T cell trafficking during an antiviral immune response. *J. Exp. Med.* 189: 1631–1638.
44. Berlin, C., R. F. Bargatze, J. J. Campbell, U. H. von Andrian, M. C. Szabo, S. R. Hasslen, R. D. Nelson, E. L. Berg, S. L. Erlandsen, and E. C. Butcher. 1995. α_4 integrins mediate lymphocyte attachment and rolling under physiologic flow. *Cell* 80: 413–422.
45. Berlin, C., E. L. Berg, M. J. Briskin, D. P. Andrew, P. J. Kilshaw, B. Holzmann, I. L. Weissman, A. Hamann, and E. C. Butcher. 1993. $\alpha_4\beta_7$ integrin mediates lymphocyte binding to the mucosal vascular addressin MAdCAM-1. *Cell* 74: 185–195.
46. Streeter, P. R., E. L. Berg, B. T. Rouse, R. F. Bargatze, and E. C. Butcher. 1988. A tissue-specific endothelial cell molecule involved in lymphocyte homing. *Nature* 331: 41–46.
47. Lindholm, C., A. Naylor, E. L. Johansson, and M. Quiding-Jarbrink. 2004. Mucosal vaccination increases endothelial expression of mucosal addressin cell adhesion molecule 1 in the human gastrointestinal tract. *Infect. Immun.* 72: 1004–1009.
48. Lundgren, A., C. Trollmo, A. Edebo, A. M. Svennerholm, and B. S. Lundin. 2005. *Helicobacter pylori*-specific $CD4^+$ T cells home to and accumulate in the human *Helicobacter pylori*-infected gastric mucosa. *Infect. Immun.* 73: 5612–5619.
49. Belyakov, I. M., S. A. Hammond, J. D. Ahlers, G. M. Glenn, and J. A. Berzofsky. 2004. Transcutaneous immunization induces mucosal CTLs and protective immunity by migration of primed skin dendritic cells. *J. Clin. Invest.* 113: 998–1007.
50. Clarke, L. L., B. R. Grubb, S. E. Gabriel, O. Smithies, B. H. Koller, and R. C. Boucher. 1992. Defective epithelial chloride transport in a gene-targeted mouse model of cystic fibrosis. *Science* 257: 1125–1128.
51. Yamamoto, S., Y. Takeda, M. Yamamoto, H. Kurazono, K. Imaoka, M. Yamamoto, K. Fujihashi, M. Noda, H. Kiyono, and J. R. McGhee. 1997. Mutants in the ADP-ribosyltransferase cleft of cholera toxin lack diarrheagenicity but retain adjuvanticity. *J. Exp. Med.* 185: 1203–1210.
52. Maghazachi, A. A., A. Al-Aoukaty, C. Naper, K. M. Torgersen, and B. Rolstad. 1996. Preferential involvement of Go and Gz proteins in mediating rat natural killer cell lysis of allogeneic and tumor target cells. *J. Immunol.* 157: 5308–5314.

Cancer Immunol Immunother
DOI 10.1007/s00262-008-0643-x

ORIGINAL ARTICLE

A possible mechanism of intravesical BCG therapy for human bladder carcinoma: involvement of innate effector cells for the inhibition of tumor growth

Tomoe Higuchi · Masumi Shimizu · Atsuko Owaki · Megumi Takahashi · Eiji Shinya · Taiji Nishimura · Hidemi Takahashi

Received: 27 June 2008 / Accepted: 8 December 2008

Abstract Intravesical bacillus Calmette-Guerin (BCG) therapy is considered the most successful immunotherapy against solid tumors of human bladder carcinoma. To determine the actual effector cells activated by intravesical BCG therapy to inhibit the growth of bladder carcinoma, T24 human bladder tumor cells, expressing very low levels of class I MHC, were co-cultured with allogeneic peripheral blood mononuclear cells (PBMCs) with live BCG. The proliferation of T24 cells was markedly inhibited when BCG-infected dendritic cells (DCs) were added to the culture although the addition of either BCG or uninfected DCs alone did not result in any inhibition. The inhibitory effect was much stronger when the DCs were infected with live BCG rather than with heat-inactivated BCG. The live BCG-infected DCs secreted TNF-α and IL-12 within a day and this secretion continued for at least a week, while the heat-inactivated BCG-infected DCs secreted no IL-12 and little TNF-α. Such secretion of cytokines may activate innate alert cells, and indeed NKT cells expressing IL-12 receptors apparently proliferated and were activated to produce cytocidal perforin among the PBMCs when live BCG-infected DCs were externally added. Moreover, depletion of $\gamma\delta$ T-cells from PBMCs significantly reduced the cytotoxic effect on T24 cells, while depletion of CD8β cells did not affect T24 cell growth. Furthermore, the innate effectors seem to recognize MICA/MICB molecules on T24 via NKG2D receptors. These findings suggest the involvement of innate alert cells activated by the live BCG-infected DCs to inhibit the growth of bladder carcinoma and provide a possible mechanism of intravesical BCG therapy.

Keywords Bladder cancer · Dendritic cells · Innate immunity · BCG · NKT cells

Introduction

Intravesical bacillus Calmette-Guerin (BCG) therapy is considered the most successful immunotherapy against solid tumors in cases of human superficial bladder carcinoma particularly in preventing from its recurrence [1, 4]. Intravesical immunotherapy with live BCG results in a massive local immune response characterized by the secretion of various cytokines in the urine [14, 27] or bladder tissue as well as by the infiltration of granulocytes and mononuclear cells into the bladder wall after repeated treatment with BCG instillation [3, 21], indicating the immunopathological responses induced at the local mucosal compartment may correlate with the BCG-mediated anti-tumor effect. However, neither the precise mechanisms nor the actual effector cells underlying the anti-tumor effect that BCG therapy stimulates remain to be elucidated.

The bladder is a confined mucosal compartment, where BCG is able to be maintained at a high concentration and thus may achieve long-lasting, continuous immune activation, which seems to better stimulate innate local immunity having broad cross-reactivity with less memory rather than acquired systemic immunity with high specificity and memory originated from rearranged genes. Therefore, live

T. Higuchi · M. Shimizu · A. Owaki · M. Takahashi · E. Shinya · H. Takahashi (✉)
Department of Microbiology and Immunology, Nippon Medical School, 1-1-5 Sendagi, Bunkyo-ku, Tokyo 113-8602, Japan
e-mail: htkuhkai@nms.ac.jp

T. Higuchi · T. Nishimura
Department of Urology, Nippon Medical School, Tokyo 113-8602, Japan

Published online: 13 January 2009

BCG appears to activate various types of innate immune effectors such as γδT lymphocytes [17, 18] and CD1 molecule-restricted lipid/glycolipid antigen-specific T cells including CD1d-restricted natural killer T (NKT) cells [12, 13] via live BCG-infected dendritic cells (DCs). Such DCs express not only peptide antigen-loaded individually restricted class I and II MHC molecules but also species-specific CD1 molecules on their surface to present BCG-derived lipid/glycolipid antigens [15, 20]. Indeed, findings that live BCG-infected DCs can be recognized by CD1 molecule-restricted but not by class I MHC molecule-restricted $CD8^+$ T cells [16] and that the Vγ2Vδ2 T lymphocytes response to BCG by immunization in macaques with live BCG [5] have recently been reported. Moreover, a close relationship between BCG-immunization, and NKT cell activation has also been shown [9]. Therefore, continuous stimulation in the confined bladder space with live BCG may activate those local innate effectors, which may control bladder cancer expansion in vivo.

The cell line T24, a well-known cell for human bladder cancer [19], expresses markedly down-modulated MHC class I molecules on the cell surface in comparison with normal peripheral blood mononuclear cells (PBMCs). Hence, the T24 line is possibly regulated by cells in a class I MHC molecule-unrelated manner rather than by the autologous class I MHC molecule-restricted conventional CD8-positive cytotoxic T lymphocytes (CTLs). Therefore, we co-cultured T24 cells with allogeneic PBMCs pretreated with live BCG to determine the actual cells activated by the BCG for controlling T24 tumor cell proliferation and elimination, and found that innate alert cells such as Vγ2Vδ2 T cells and particularly NKT cells derived from allogeneic PBMCs activated by the live BCG-pretreated DCs appear to inhibit the proliferation of T24 tumor cells as well as eliminate them. The findings shown in the present study strongly suggest the involvement of innate alert effectors in controlling bladder cancer growth and shed light on the actual feature of the mechanisms for the anti-tumor effect of intravesical BCG therapy.

Materials and methods

Cell lines

Human urinary bladder carcinoma T24 cells (ATCC HTB-4) were cultured in McCoy's 5a medium (Invitrogen, Carlsbad, CA) supplemented with 10% FCS (HyClone Laboratories, Logan, UT), 50 U/ml penicillin (Invitrogen), and 50 mg/ml streptomycin (Invitrogen). Human colon cancer derived HCT116 cells (ATCC CCL 247), C1R cells were cultured in Dulbecco's modified Eagle's medium (Sigma-Aldrich, St Louis, MO) supplemented with 10% FCS (HyClone), 50 U/ml penicillin, and 50 mg/ml streptomycin (Invitrogen). Myelogenous leukemia K562 cells, and T lymphoblast Jurkat cells were cultured in RPMI 1640 (Sigma-Aldrich, St Louis, MO)-based complete T-cell medium (CTM) [25] supplemented with 10% FCS, 2 mM L-glutamine (ICN Biomedicals, Aurora, OH), 100 units/ml penicillin, 100 μg/ml streptomycin, 1 mM HEPES (Invitrogen), 1 mM sodium pyruvate (Invitrogen), 50 mM 2-mercaptoethanol (2-ME) (Invitrogen).

Infection of DCs with live or heat-inactivated BCG

A lyophilized preparation of BCG, the Tokyo 172 strain (12 mg dry weight per ample) (Japan BCG Laboratory, Tokyo, Japan) was used to carry out the experiments. For the infection experiments, BCG was harvested at a mid-log growth phase, washed, and suspended in RPMI 1640 medium supplemented with 10% FCS. The suspension was passed through a 5-μm pore size filter to obtain single-cell bacteria. The viability of bacteria was constantly >90%. The BCG preparation was divided into two equal aliquots; one incubated for 30 min at 85°C to kill the bacteria and the other left at room temperature as reported recently [16].

Generation of DCs from PBMCs and their treatment with BCG

DCs were obtained from PBMCs as described recently [26]. In brief, PBMCs were freshly isolated with Ficoll-Hypaque (Amersham-Pharmacia Biotech, Uppsala, Sweden) from peripheral blood of healthy volunteers, and $CD14^+$ monocytes were immediately separated by magnetic depletion using a monocyte isolation kit (Miltenyi Biotec, Bergisch Gladbach, Germany) containing hapten-conjugated antibodies to CD3, CD7, CD19, CD45RA, CD56, and anti-IgE Abs and a magnetic cell separator (MACS, Miltenyi Biotec) according to the manufacturer's instructions, routinely resulting in >90% purity of $CD14^+$ cells. Cells were cultured in 24-well plates for 6–7 days in CTM supplemented with 200 ng/ml GM-CSF (PeproTech, Rocky Hill, NJ), and 10 ng/ml IL-4 (Biosource Intl., Camarillo, CA) to obtain DCs. For the treatment with BCG, 1×10^5 DCs in 1 ml of CTM were incubated overnight with 0.1 mg of either live BCG or heat-inactivated BCG. After being washed three times with RPMI1640 medium, the BCG-treated DCs were further co-cultured with 1×10^6 PBMCs of the same donor to carry out the experiments.

Antibodies and flow-cytometric analysis

Fluorescein isothiocyanate (FITC)-conjugated anti-human monoclonal antibodies (mAbs) to mouse IgG1κ, isotype control (MOP-21), HLA-ABC (G46-2.6), CD3 (H1T3a),

CD161 (DX12), CD80 (B7-1) (L307.4), CD86 (B70/B7-2) [2331(FUN-1)], as well as phycoerythrin (PE)-conjugated mouse IgG1κ, isotype control, CD3, CD56 (B159), and unlabeled anti-human CD3, CD4 (RPA-T4), Vδ2 (B6), and CD161, were all purchased from BD Biosciences (San Diego, CA). Unlabeled anti-human CD8β (2ST8.5H7) mAb was purchased from IMMUNOTECH (Marseille, Cedex, France). Cells were stained with the relevant antibody on ice for 30 min in phosphate-buffered saline (PBS) with 2% FCS and 0.01 M sodium azide (PBS-based medium), washed twice, and re-suspended in the PBS-based medium. Then, the labeled cells were analyzed with a FACScan (BD Biosciences) using CellQuest software (BD Biosciences). Live cells were gated based on propidium iodide gating.

Depletion of cells from PBMCs

To deplete Vδ2-positive cells, PBMCs were incubated with mouse anti-human Vδ2 mAb (B6) for 30 min at 4°C and washed three times to remove free mAb. Then the stained cells were further incubated with magnetic beads-conjugated anti-mouse IgG (Dynabeads Pan Mouse IgG) (DYNAL BIOTECH, Oslo, Norway), and Vδ2-positive cells were eliminated by magnetic device (Perspective Biosystems, Framingham, MA) following the manufacturer's instruction. CD8β, CD3, CD161, and CD4-positive cells were also depleted using the same procedure.

Quantification of cytokine production from BCG-treated DCs by ELISA

Monocyte-derived DCs (1×10^6) were incubated with 1 ml of CTM containing 0.1 mg of BCG in 24-well culture plate for 2–3 days and the culture supernatants were collected and stored at −80°C until the measurement of cytokines. Production of TNF-α, IL-12, IL-10, and IL-4 was measured using the DuoSet ELISA Development Kit (R&D systems, Minneapolis, MN) according to the manufacturer's instructions.

Chromium-51 release assay

The cytotoxicity of BCG-activated cells was measured by a standard 4-h ^{51}Cr-release assay using T-24 human bladder cancer cells or NK-sensitive K562 myelogenous leukemia cells as targets. In brief, various numbers of effector cells were incubated with 3×10^3 ^{51}Cr-labeled targets for 4 h at 37°C in 200 μl of RPMI 1640 medium containing 10% FCS in round-bottomed 96-well cell culture plates (BD Biosciences). After incubation, the plates were centrifuged for 10 min at 330×*g*, and 100 μl of cell-free supernatant was collected to measure radioactivity with a Packard Auto-Gamma 5650 counter (Hewlett-Packard Japan, Tokyo, Japan). Maximum release was determined from the supernatant of cells that had been lysed by the addition of 5% Triton ×-100 and spontaneous release was determined from target cells incubated without added effector cells. The percent specific lysis was calculated as 100× (experimental release – spontaneous release)/(maximum release – spontaneous release). Standard errors of the means of triplicate cultures were always <5% of the mean. Data are expressed as the mean ± SEM. Each experiment was performed at least three times.

T24 growth inhibition assay

The T24 growth inhibition assay was performed by incubating 1×10^4 T24 cells with 5×10^4 or 1×10^5 freshly isolated allogeneic PBMCs in 200 μl of CTM for 3 days at 37°C in 5% CO_2 based on a recent study [22]. Samples were cultured in triplicate on 96-well U-bottom plates. The cells were then labeled for 16 h with 1 μCi/well of tritiated thymidine (^{3}H-TdR; MP Biomedicals, Morgan, CA), harvested in an automated plate harvester (TomTech, Orange, CT), and counted in a 1,450 Micro Beta TRILUX scintillation spectrometer (Wallac, Gaithersburg, MD). Data are expressed as the mean count per minute (cpm) ± SEM.

RT-PCR for CD1d mRNA in T24 cells

Total RNA was extracted from T24, Jurkat, and HCT cells using the RNeasy Protocol Mini Kit (Qiagen, Valencia, CA) according to the manufacturer's instructions. RNA (2 μg) was reverse transcribed with oligo-(dT)18 (Perkin Elmer, Wellesley) priming and Superscript III (Invitrogen) reverse transcriptase in a 20 μg reaction mixture at 50°C for 60 min. A measure of 1 μl (equal to about 200 ng) of the cDNA product was then subjected to 30 cycles of 30 s at 94°C, 1 min at 64°C, and 1 min final extension at 72°C, with a thermocycler (PCR express; Hybaid, Teddington, Middlesex, UK). The amplification was performed in a reaction volume of 20 μl with LA PCR buffer (Takara, Shiga, Japan), composed of 2.5 mM $MgCl_2$, 0.3 nM of each deoxynucleotide triphosphate, 2.5 mM of each primer, and 1 U of LA Taq polymerase (Takara). The following oligonucleotide primers were designed from the published cDNA sequence [6]: GAPDH sense-primer (5′-GCCTCAA GATCATCAGCAATGC-3′) and antisense-primer (5′-AT GCCAGTGAGCTTCCCGTTC-3′), human CD1d (hCD1d) full-length sense-primer (5′-CGGGATCCATGGGGTGC CTGCTGTTTCTG-3′), antisense-primer (5′-ATTTGCGG CCGCCAGGACGCCCTGAT-3′), hCD1d short fragment sense-primer (5′-CTCCAGATCTCGTCCTTCGCCATT-3′), antisense-primer (5′-TTGAATGGCCAAGTTTACCCAA AG-3′).

Measurement of cytotoxicity by BCG-activated innate effctors through NKG2D-receptor against MICA/MICB molecules on T24 tumor cells

Cytotoxicity of innate effectors activated by live BCG-treated DC against T24 cells was investigated using 51-chromium release assay shown above in the presence of various blocking antibodies such as anti-human MICA/MICB (6D4) (BioLegend, San Diego, CA), anti-human NKG2D (CD314)-specific mouse mAbs (1D11) (BioLegend), or isotype-matched control mouse IgG1κ (BD Biosciences). $CD3^+CD56^+$ NKT cells were sorted out with FACS-Vantage SE (BD Biosciences) according to the manufacturer's instruction.

Results

T24 growth inhibition by allogeneic PBMCs activated with live BCG-treated DCs

The bladder cancer cell line T24, a well-known cell for human bladder cancer, expresses markedly reduced levels of MHC class I molecules on the cell surface in comparison with normal PBMCs (data not shown). Thus, the T24 line is possibly regulated by cells in a class I MHC molecule-unrelated manner rather than by the autologous class I MHC molecule-restricted conventional CTLs. Therefore, we used allogeneic PBMCs to gain insight into the actual cells activated by BCG for controlling T24 tumor cell proliferation and elimination.

When 5×10^4 or 1×10^5 freshly isolated allogeneic PBMCs were co-cultured with 1×10^4 T24 cells in the presence of live BCG, strong inhibition of T24 cell proliferation measured with ^{3}H-TdR was observed as compared with BCG-absent control (Fig. 1a). Because the BCG-susceptible cells are thought to be DCs, DCs from the PBMCs were pretreated with (0.1 mg/ml) live BCG for 6 h at 37°C. Then, after confirmation that the addition of live BCG-pretreated DCs alone did not affect the T24 cell proliferation, 1×10^4 T24 cells were incubated with an equal number of the indicated DCs together with 5×10^4 or 1×10^5 allogeneic PBMCs of the same donor. Profound inhibition of T24 cell proliferation was observed when live BCG-infected DCs were co-cultured with PBMCs of the same donor (Fig. 1b). Moreover, the effect of live or heat-inactivated BCG-treated DCs on T24 cell proliferation was also examined. As indicated in Fig. 1c, the addition of heat-inactivated BCG-pretreated DCs resulted in partial inhibition of the proliferation. These results indicated that some cells derived from allogeneic PBMCs activated by the live BCG-pretreated DCs might gain the capacity to inhibit the proliferation of T24 tumor cells.

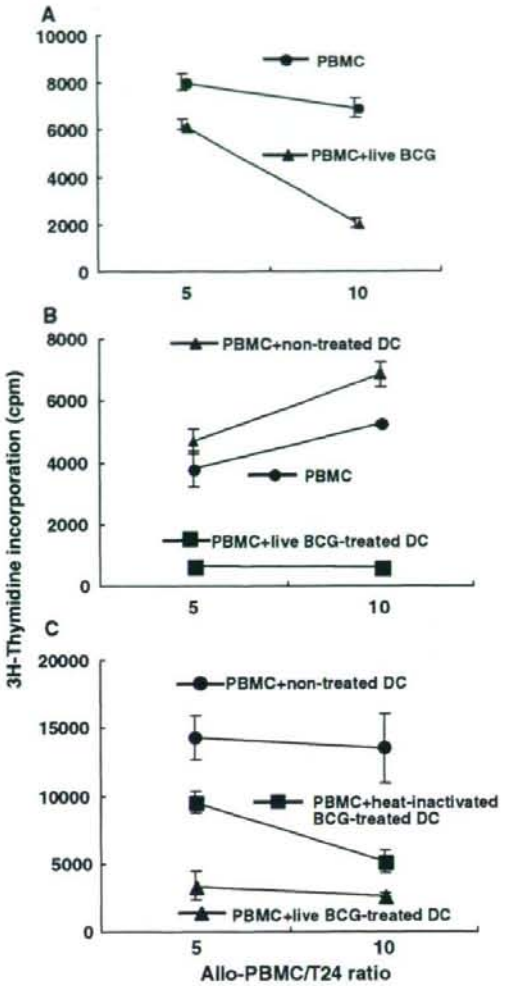

Fig. 1 Inhibition of T24 growth by allogeneic PBMCs activated with live BCG-treated DCs. **a** When 5×10^4 or 1×10^5 freshly isolated allogeneic PBMCs were co-cultured with 1×10^4 T24 cells in the presence of live BCG (*closed triangle*), strong inhibition of T24 cell proliferation measured by ^{3}H-TdR was observed in comparison with the BCG-absent control (*closed circle*). **b** T24 cells (1×10^4) were incubated with 5×10^4 or 1×10^5 allogeneic PBMCs. Profound inhibition of T24 cell proliferation was observed when live BCG-infected DCs were co-cultured with PBMCs (*closed square*). However, no inhibition was observed when T24 cells were co-cultured either with PBMC alone (*closed circle*) or with PBMC plus BCG-uninfected DCs (*closed triangle*). **c** T24 cells (1×10^4) were incubated with 5×10^4 or 1×10^5 allogeneic PBMCs plus live BCG-treated DCs (*closed triangle*), heat-inactivated BCG-treated DCs (*closed square*), or control untreated DCs (*closed circle*). Again, strong inhibition of T24 cell proliferation was observed when PBMCs were co-cultured with live BCG-infected DCs (*closed triangle*) and partial inhibition was seen when they were co-cultured with heat-inactivated BCG-treated DCs (*closed square*)

Kinetics of cytokine secretion by live BCG-treated DCs

Next, the live BCG-treated DCs were compared with the inactivated BCG-treated DCs in terms of the kinetics of cytokine secretion. As demonstrated in Fig. 2a with closed columns, live BCG-treated DCs secreted quite a large amount of IL-12 2–3 days after the incubation, however, heat-inactivated BCG-treated DCs shown with open columns secreted almost no detectable amount of IL-12. As for TNF-α, live BCG-treated DCs secreted more of it than heat-inactivated BCG-treated DCs (Fig. 2b). In contrast, the amount of IL-10 secretion was almost the same between the two (Fig. 2c). Furthermore, the expression levels of co-stimulated molecules, CD80 and CD86, were higher in live BCG-treated DCs (data not shown).

T24 growth inhibition was mainly mediated through CD8β-negative T cells

These findings suggest live BCG-activated DCs to activate effectors from PBMCs to inhibit T24 cell proliferation through the secretion of IL-12 and TNF-α. Therefore, to examine the actual cells that eliminate T24, CD3-positive T cells were eliminated from among the activated PBMCs with live BCG-treated DCs, and the cytotoxicity against ^{51}Cr-labeled T24 targets was measured. The cytotoxicity was significantly reduced by the elimination of the CD3-positive cells (Fig. 3a). The remaining weak cytotoxicity, shown as open circles in Fig. 3a, might be due to the effect of activated non-T cells such as NK cells. Moreover, the cytotoxicity against T24 cells was not inhibited by the elimination of CD8β-positive cells (shown as closed squares) (Fig. 3b). These results suggest that the class I MHC molecule-restricted conventional CD8β-positive CTL do not seem to be involved in this T24-related cytotoxicity.

T24 tumor growth was partially inhibited by Vγ2Vδ2 T cells

Collectively, the cytotoxity against T24 cells mediated through live BCG-treated DCs appeared to be provided by the major effectors of innate immunity; NK cells, NKT cells, and γδ T cells. Thus, we then examined the possible involvement of γδT cell effectors in the elimination of tumor cells. γδ T cells are classified into two distinct types, type-1 expressing Vγ1Vδ1 T-cell receptor (TCR) and type-2 expressing Vγ2Vδ2 TCR, with the majority of cells generated by BCG reported to be the latter type-2 γδ T cells [11]. When the Vδ2-positive type-2 γδT cells were eliminated from live BCG-activated PBMCs, slight inhibition of the cytotoxicity against T24 cells was observed and this was apparent when the Vδ2-positive cells were depleted from PBMCs before co-culturing with BCG-treated DCs

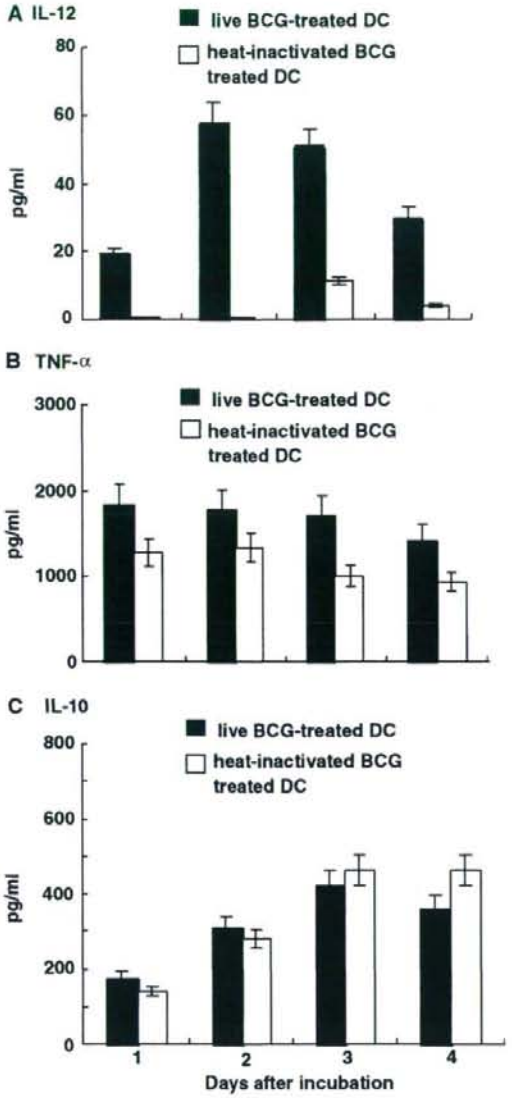

Fig. 2 Measurement of cytokine production by BCG-treated DCs. The difference in the kinetics of cytokine secretion between live BCG-treated DCs and inactivated BCG-treated DCs was compared. Live BCG-treated DCs (*closed column*) secreted predominantly large amounts of IL-12 (**a**) and larger amounts of TNF-α (**b**) than heat-inactivated BCG-treated DCs (*open column*), while the amount of IL-10 secretion (**c**) was lower than in the case of heat-inactivated BCG-treated DCs

(Fig. 3c). Moreover, PBMCs treated with risedronate, an activator of Vδ2 [8], showed strong anti-tumor effect against T24 cells (Fig. 3d). These results indicate the involvement of live BCG-activated Vγ2Vδ2 TCR-expressing type-2 γδT cells in the elimination of T24 tumor cells.

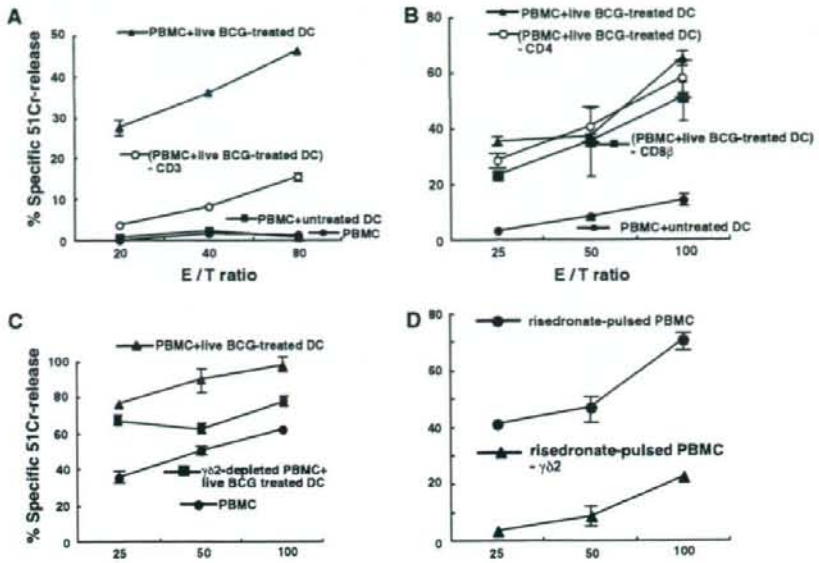

Fig. 3 T24 growth inhibition was partially mediated through CD8β-negative Vγ2Vδ2 T cells. **a** When CD3-positive T cells were eliminated from among the activated PBMCs with live BCG-treated DCs, the cytotoxicity against T24 tumor cells was significantly reduced (*open circle*) almost to the basal level mediated by normal PBMC (*closed circle*) or PBMC plus untreated DCs (*closed square*) in comparison with positive PBMCs activated with live BCG-treated DCs (*closed triangle*) and the remaining weak cytotoxicity might be due to the effect of activated non-T cells such as NK cells. **b** Such cytotoxicity against T24 cells was not abrogated by the elimination of CD8β-positive cells (*closed square*). The results suggest the class I MHC molecule-restricted conventional CD8β-positive CTLs do not seem to be involved in this T24-related cytotoxicity. The elimination of CD4-positive cells (*open circle*) from live BCG-activated PBMCs (*closed triangle*) did not result in any reduction of cytotoxicity against T24 targets in comparison with the basal level mediated by normal PBMC plus untreated DCs (*closed circle*). **c** When the Vδ2-positive cells were depleted from PBMCs before co-culturing with live BCG-treated DCs (*closed square*), the cytotoxicity against T24 was apparently reduced nearly by half in comparison with PBMCs activated with live BCG-treated DCs (*closed triangle*). **d** Moreover, the Vδ2 cell-enriched population from PBMCs co-cultured with risedronate showed a strong anti-tumor effect against T24 cells (*closed circle*). The elimination of type-2 $\gamma\delta$T cells resulted in a significant reduction in the cytotoxicity against T24 cells (*closed triangle*). These results indicate the involvement of live BCG-activated Vγ2Vδ2 TCR-expressing type-2 $\gamma\delta$T cells in the elimination of T24 tumor cells

Effect of depletion of CD161-positive cells on T24 growth

CD161 is known as a marker for NK and NKT cells. Thus, to examine the effect of NK and NKT cells on the elimination of T24 cells, CD161-positive cells were depleted from PBMCs activated by live BCG-treated DCs, and their elimination was confirmed by flowcytometry (Fig. 4a). After confirming that the CD161-positive cells were depleted, the cytotoxicity of the remaining cells against T24 cell was measured by ^{51}Cr-release assay. A profound reduction in the cytotoxity was observed when the CD161-positive cells were eliminated and the reduced cytotoxicity was slightly greater than that of the activated PBMCs co-cultured with live BCG-treated DCs (Fig. 4b). These findings suggest the residual $\gamma\delta$T cells after the elimination of CD161-positive cells to be slightly more cytotoxic than the activated NK cells in PBMCs. Also, as shown in Fig. 4c, that the live BCG-activated PBMCs showed far stronger cytotoxicity than untreated PBMCs against K562 cells that are known to be sensitive to NK cells indicates NK cells to be less cytotoxic to T24 tumor cells than innate $\gamma\delta$T or NKT cells. Taken together, these results suggest the most potent effectors among the live BCG-activated cells against T24 seem to be NKT cells.

Significant production and increase of perforin in the NKT cell population among PBMCs co-cultured with live BCG-treated DCs

Thus, to confirm the actual number and increase of NKT cells among PBMCs co-cultured with live BCG-treated DCs, a flow-cytometric analysis was performed. The results showed that the number of both $CD3^+CD56^+$ cells and $CD3^+CD161^+$ NKT cells but not $CD3^-CD56^+$ or $CD3^-CD161^+$ NK cells apparently increased among those PBMCs activated by live BCG-treated DCs but not by heat-

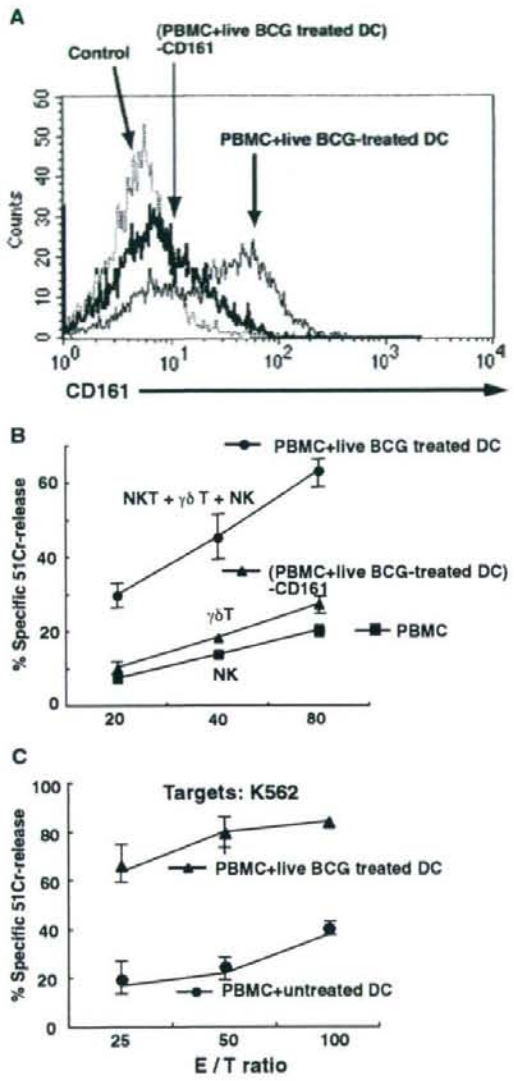

Fig. 4 Effect of CD161 positive cells depletion on T24 growth. **a** The elimination of CD161-positive cells was confirmed by flow cytometry. **b** The remaining cells after the elimination of CD161-positive cells (*closed triangle*) showed a profound reduction of cytotoxicity against T24 cells compared to live BCG-activated PBMCs (*closed circle*). The findings suggest that the residual γδT cells after the elimination of CD161-positive cells had slightly stronger cytotoxicity than the activated NK cells in PBMCs (*closed square*). **c** PBMCs activated by live BCG-treated DCs (*closed triangle*) showed far stronger cytotoxicity than BCG-untreated PBMCs (*closed circle*) against NK-sensitive K562 cells. These results indicate that NK cells have weaker cytotoxicity against T24 tumor cells than innate γδT or NKT cells activated by live BCG-treated DCs

inactivated BCG-treated DCs (Fig. 5a). Therefore, the number of NKT cells certainly increased in the live BCG-activated population. Moreover, those live BCG-activated NKT cells actually produced to secrete cytocidal molecules like perforin (Fig. 5b) or granzyme B (data not shown). Also, it should be noted that the live BCG-activated γδT cells became effector/memory state expressing CD45RO from naïve state expressing CD45RA although the number of γδT cells did not altered (data not shown).

Increased NKT cells inhibited T24 cells in a CD1d-unrestricted fashion

In general, NKT cells recognize glycolipid antigens presented by CD1d [23]. To clarify whether the live BCG-activated NKT cells see T24 tumor antigens in a CD1d-restricted manner, the expression of CD1d on T24 cells was investigated. Despite careful and intense examination, neither mRNA encoding CD1d nor the surface expression of CD1d was detected in not only untreated T24 cells but also BCG-treated ones (Fig. 6a, b), indicating that T24 will not express CD1d molecules even incorporating BCG into their cellular component.

Therefore, to exclude the possibility of subtle expression for functional CD1d on T24 cells after the BCG treatment, an established human NKT line (HT-AC2) that recognizes α-galactosyl ceramide (α-GalCer) and secretes IL-4 in a CD1d-restricted manner (Shimizu & Takahashi, manuscript in preparation) and C1R/CD1d cells expressing human CD1d gene, we examined whether NKT cells can recognize T24 cells in the presence of α-GalCer. No IL-4 was detected in the supernatant of the NKT cell line co-cultured with α-GalCer-pulsed T24 as well as BCG-treated T24 cells (Fig. 6c). Collectively, NKT cells but not NK cells induced by the live BCG-activated DCs seem to predominantly eliminate or suppress T24 tumor cells in a CD1d-unrestricted, α-GalCer independent fashion.

Possible tumor cell ligands for BCG-activated NKT cell recognition

Because NKG2D expression was observed on the NKT cells or γδT cells expanded from live BCG-treated PBMCs (data not shown), blocking effect of antibodies for stress-associated tumor cell-specific molecules such as MICA/MICB [2, 10], the counterparts of NKG2D receptor, on the recognition of T24 cells was examined based on the recent finding [28]. As demonstrated in Fig. 7a, significant inhibition of the cytotoxicity mediated by activated NKT cells was seen when anti-MICA/MICB specific antibody was added, although isotype-

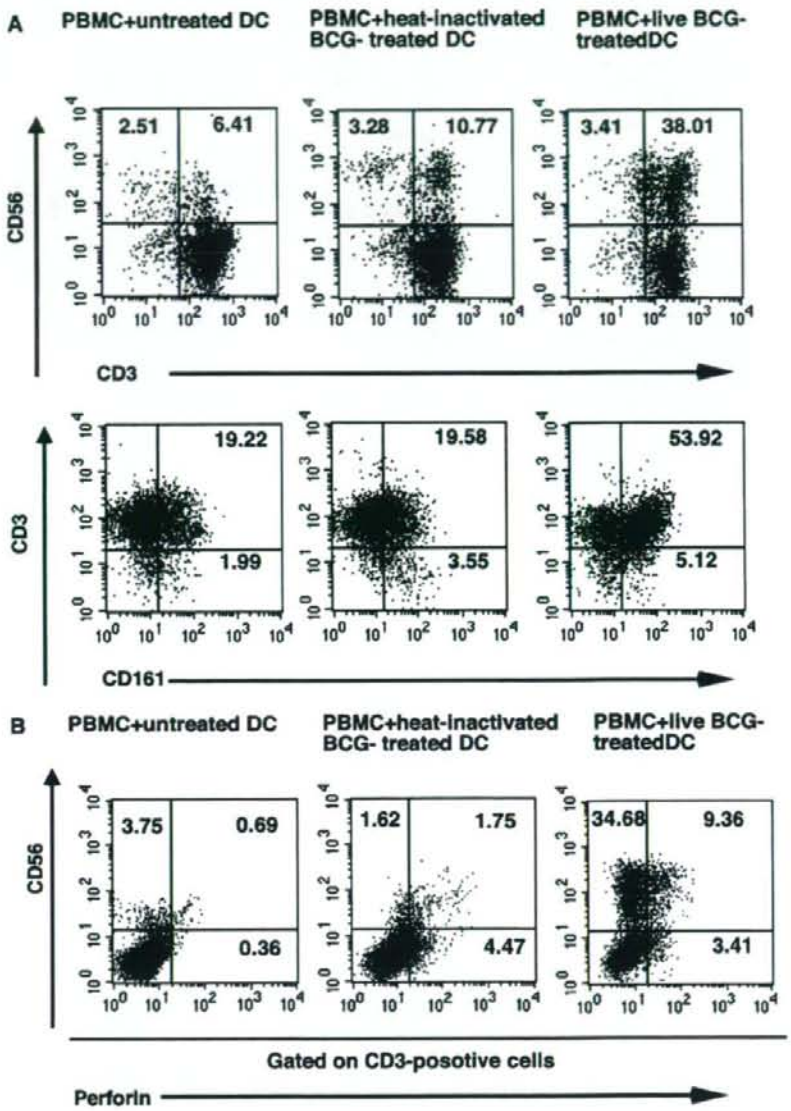

Fig. 5 Significant increase and perforin production in the number of NKT cells among PBMCs activated by live BCG-treated DCs. a Flow-cytometric analysis showed that the number of both $CD3^+CD56^+$ cells, and $CD3^+CD161^+$ NKT cells but not $CD3^-CD56^+$ or $CD3^-CD161^+$ NK cells apparently increased among those PBMCs activated by live BCG-treated DCs but not by heat-inactivated BCG-treated DCs. Therefore, the number of NKT cells certainly increased in the live BCG-activated population. b The live BCG-activated NKT cells actually produced to secrete cytocidal molecules like perforin, while heat-inactivated BCG-associated NKT did not

matched antibody did not show any inhibition for their cytotoxicity. Moderate inhibition was also seen when the NKG2D receptors blocked by their specific antibody (Fig. 7a). Similarly, cytotoxicity against T24 cells by live BCG-treated PBMCs containing mostly activated NKT cells as well as some $\gamma\delta$T and NK cells was markedly inhibited by anti-MICA/MICB specific antibody (Fig. 7b). Therefore, MICA/MICB molecules on the T24 cells appear to be a possible tumor cell ligands for BCG-activated innate NKT cell recognition.

Discussion

Intravesical BCG therapy is probably the most effective immunotherapy for recurrent superficial bladder cancer. As far as we have examined, the anti-tumor effect does not appear to be due to direct cytotoxicity of BCG itself. In fact, it was recently reported that the treatment of the urothelial carcinoma cell line T24 with BCG did not induce apoptosis, and BCG inhibited camptothecin-mediated apoptosis [7]. Similarly, treatment of T24 cells with BCG

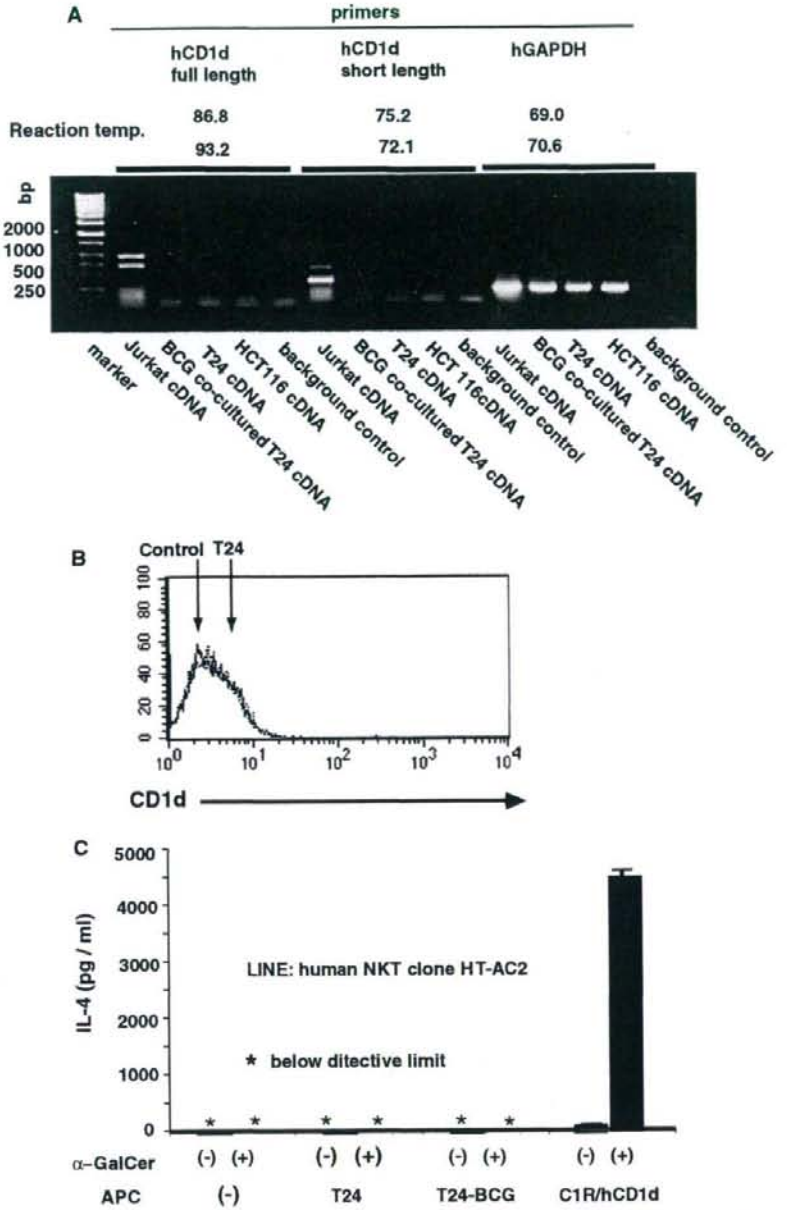

Fig. 6 Inhibition of T24 tumor growth by the BCG-activated NKT cells was mediated in a CD1d-unrestricted manner. NKT cells are usually recognized as antigens in association with CD1d molecules. Thus, **a** both internal mRNA for CD1d expression and **b** external surface expression were examined in T24 tumor cells. However, CD1d expression could not be detected at all even after co-cultured with live BCG. **c** Therefore, using an established human NKT line (HT-AC2) that recognizes α-galactosyl ceramide (α-GalCer) in a CD1d-restricted manner and secretes IL-4 (Shimizu & Takahashi, manuscript in preparation) and CD1d-expressing C1R cells (C1R/hCD1d), we investigated whether NKT cells can recognize live BCG-treated (T24-BCG) or untretaed T24 cells in the presence of α-GalCer. No IL-4 was detected in the supernatant of NKT cells co-cultured with α-GalCer-pulsed those T24 cells. Taken together, NKT cells generated by the live BCG-activated DCs seem to inhibit T24 tumor cell growth in a CD1d-unrestricted manner

did not cause any apoptotic changes as examined with a TUNEL assay [24]. Therefore, BCG itself does not eliminate T24 tumor cells but rather some immune system activated by BCG may indirectly inhibit the growth of these cells or eliminate them.

The body has two distinct immune systems to suppress tumor growth or eliminate tumor cells. One is systemic acquired immunity with highly specific effectors such as class I MHC molecule-restricted $CD8^+$ CTLs, class II MHC molecule-restricted $CD4^+$ T cells, and specific antibodies. These effectors express specific receptors originating from rearranged genes established by periodic stimulation. The magnitude of specific responses will increase synergistically with the number of stimulations.

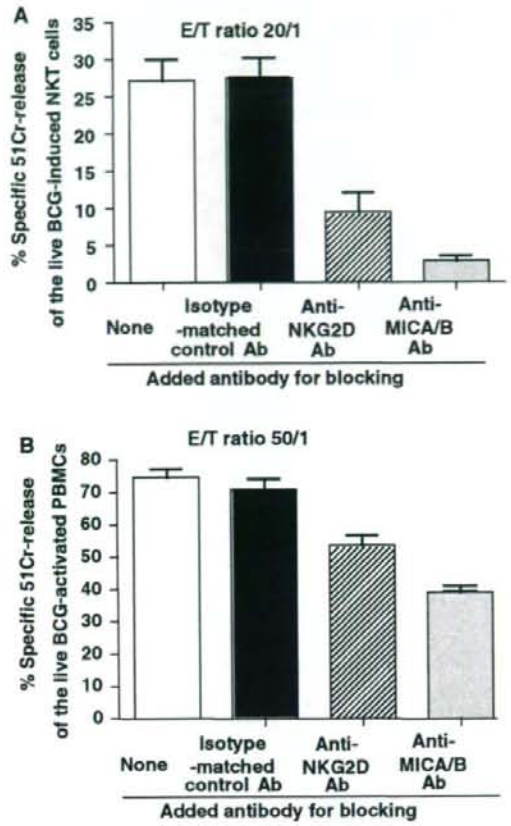

Fig. 7 Possible tumor cell ligands for BCG-activated NKT cell recognition. **a** Effect of antibodies for blocking stress-associated tumor cell-specific molecules such as MICA/MICB, the counterparts of NKG2D receptor, on the recognition of T24 cells was examined. Significant inhibition of the cytotoxicity mediated by activated NKT cells was seen when anti-MICA/MICB specific antibody was added, although isotype-matched antibody did not show any inhibition for their cytotoxicity. Moderate inhibition was also seen when the NKG2D receptors blocked by their specific antibody. **b** Cytotoxicity against T24 cells by live BCG-treated PBMCs containing mostly activated NKT cells as well as some $\gamma\delta$T cells and NK cells was also markedly inhibited by anti-MICA/MICB specific antibody

In contrast, local innate immunity involves toll-like receptors (TLR), $\gamma\delta$ TCR, or invariant NKT–TCR having diverse cross-reactivity without requiring the strict gene-rearrangement seen in the establishment of acquired immune receptors and their activation can be maintained by constant stimulation.

Also, as has been indicated, the bladder cancer cell line T24 expresses markedly down-modulated MHC class I molecules on its surface and the expression did not recover by the treatment with live BCG or live BCG-infected DCs. Thus, the T24 tumor would be recognized in a MHC molecule-unrestricted manner. Hence, we co-cultured the T24 cells with allogeneic PBMCs in the presence of live BCG and found a profound inhibition of tumor growth in vitro. A similar strong inhibition of T24 cell proliferation was observed when live BCG-infected DCs were co-cultured with PBMCs of the same donor. Moreover, the elimination of T24 cells was achieved mostly by CD3-positive innate effectors such as Vγ2Vδ2 TCR-expressing $\gamma\delta$T cells and NKT cells having predominant cytotoxicity, but not by class I MHC molecule-restricted conventional CD8β-positive CTLs, and the innate effectors were activated by live BCG-infected DCs rather than heat-inactivated BCG-treated DCs. Furthermore, the number of NKT cells but not $\gamma\delta$T cells or NK cells certainly increased in the live BCG-activated population.

These results strongly suggest that cells that control T24 tumor growth are not conventional class I MHC molecule-restricted CD8$^+$ CTL in the acquired arm but rather MHC molecule-unrestricted $\gamma\delta$T and NKT cells in the innate arm through the activation of DCs by live BCG. The results are reasonable in that continuous stimulation in the limited confined mucosal compartment of the bladder by a live organism may activate local innate effectors. Although the possible involvement of acquired effectors like CD8$^+$ CTLs in the prevention of surface bladder tumor expansion by intravesical BCG therapy has not be excluded, the data obtained in the present study strongly indicate a dominant effect of innate cells on tumor recurrence at the confined mucosal surface. Moreover, the cytotoxic effect of innate NKT or $\gamma\delta$T cells on T24 tumor cells was mediated thought stress-associated tumor-specific MICA/MICB molecules via their NKG2D receptors but not CD1d molecule-restricted invariant NKT-TCRs, indicating that these invariant TCRs are required mainly for their activation.

If this is the actual reason why intravesical BCG therapy is most successful immunotherapy against solid tumors in terms of preventing recurrence, we must focus on the constant activation of innate immunity for the treatment of other solid tumors and preventing their spread by metastasis. The findings shown in the present study will open the new notion that constant stimulation of innate effectors such as MHC molecule-unrestricted $\gamma\delta$T and NKT cells with live microorganisms like BCG through the activation of local DCs may provide a novel therapeutic way for cancer treatment.

Acknowledgments This work was supported in part by grants from the Ministry of Education, Science, Sport, and Culture, from the Ministry of Health and Labor and Welfare, Japan, and from the Japanese Health Sciences Foundation, and by the Promotion and Mutual Aid Corporation for Private School of Japan.

References

1. Alexandroff AB, Jackson AM, O'Donnell MA, James K (1999) BCG immunotherapy of bladder cancer: 20 years on. Lancet 353:1689–1694
2. Bauer S, Groh V, Wu J, Steinle A, Phillips JH, Lanier LL, Spies T (1999) Activation of NK cells and T cells by NKG2D, a receptor for stress-inducible MICA. Science 285:727–729
3. Bohle A, Gerdes J, Ulmer AJ, Hofstetter AG, Flad HD (1990) Effects of local bacillus Calmette-Guerin therapy in patients with bladder carcinoma on immunocompetent cells of the bladder wall. J Urol 144:53–58
4. Bohle A, Brandau S (2003) Immune mechanisms in bacillus Calmette-Guerin immunotherapy for superficial bladder cancer. J Urol 170:964–969
5. Cairo C, Hebbeler AM, Propp N, Bryant JL, Colizzi V, Pauza CD (2007) Innate-like gammadelta T cell responses to mycobacterium bacille Calmette-Guerin using the public V gamma 2 repertoire in Macaca fascicularis. Tuberculosis (Edinb) 87:373–383
6. Calabi F, Jarvis JM, Martin L, Milstein C (1989) Two classes of CD1 genes. Eur J Immunol 19:285–292
7. Chen F, Zhang G, Cao Y, Payne R, See WA (2007) Bacillus Calmette-Guerin inhibits apoptosis in human urothelial carcinoma cell lines in response to cytotoxic injury. J Urol 178:2166–2170
8. Das H, Wang L, Kamath A, Bukowski JF (2001) Vgamma2Vdelta2 T-cell receptor-mediated recognition of aminobisphosphonates. Blood 98:1616–1618
9. Emoto M, Emoto Y, Buchwalow IB, Kaufmann SH (1999) Induction of IFN-gamma-producing CD4+natural killer T cells by mycobacterium bovis bacillus Calmette-Guerin. Eur J Immunol 29:650–659
10. Groh V, Wu J, Yee C, Spies T (2002) Tumour-derived soluble MIC ligands impair expression of NKG2D and T-cell activation. Nature 419:734–738
11. Gumperz JE, Brenner MB (2001) CD1-specific T cells in microbial immunity. Curr Opin Immunol 13:471–478
12. Harada M, Magara-Koyanagi K, Watarai H, Nagata Y, Ishii Y, Kojo S, Horiguchi S, Okamoto Y, Nakayama T, Suzuki N, Yeh WC, Akira S, Kitamura H, Ohara O, Seino K, Taniguchi M (2006) IL-21-induced Bepsilon cell apoptosis mediated by natural killer T cells suppresses IgE responses. J Exp Med 203:2929–2937
13. Ishii R, Shimizu M, Nakagawa Y, Shimizu K, Tanaka S, Takahashi H (2004) In vivo priming of natural killer T cells by dendritic cells pulsed with hepatoma-derived acid-eluted substances. Cancer Immunol Immunother 53:383–390
14. Jackson AM, Alexandroff AB, Kelly RW, Skibinska A, Esuvaranathan K, Prescott S, Chisholm GD, James K (1995) Changes in urinary cytokines and soluble intercellular adhesion molecule–1 (ICAM-1) in bladder cancer patients after bacillus Calmette-Guerin (BCG) immunotherapy. Clin Exp Immunol 99:369–375
15. Kaufmann SH (2004) New issues in tuberculosis. Ann Rheum Dis 63(Suppl 2):ii50–ii56
16. Kawashima T, Norose Y, Watanabe Y, Enomoto Y, Narazaki H, Watari E, Tanaka S, Takahashi H, Yano I, Brenner MB, Sugita M (2003) Cutting edge: major CD8 T cell response to live bacillus Calmette-Guerin is mediated by CD1 molecules. J Immunol 170:5345–5348
17. Lee J, Choi K, Olin MR, Cho SN, Molitor TW (2004) Gammadelta T cells in immunity induced by mycobacterium bovis bacillus Calmette-Guerin vaccination. Infect Immun 72:1504–1511
18. Martino A, Casetti R, Sacchi A, Poccia F (2007) Central memory Vgamma9Vdelta2 T lymphocytes primed and expanded by bacillus Calmette-Guerin-infected dendritic cells kill mycobacterial-infected monocytes. J Immunol 179:3057–3064
19. O'Toole CM, Povey S, Hepburn P, Franks LM (1983) Identity of some human bladder cancer cell lines. Nature 301:429–430
20. Porcelli SA, Modlin RL (1999) The CD1 system: antigen-presenting molecules for T cell recognition of lipids and glycolipids. Annu Rev Immunol 17:297–329
21. Prescott S, James K, Hargreave TB, Chisholm GD, Smyth JF (1992) Intravesical Evans strain BCG therapy: quantitative immunohistochemical analysis of the immune response within the bladder wall. J Urol 147:1636–1642
22. Pryor K, Stricker P, Russell P, Golovsky D, Penny R (1995) Antiproliferative effects of bacillus Calmette-Guerin and interferon alpha 2b on human bladder cancer cells in vitro. Cancer Immunol Immunother 41:309–316
23. Saito N, Takahashi M, Akahata W, Ido E, Hidaka C, Ibuki K, Miura T, Hayami M, Takahashi H (2005) Analysis of evolutionary conservation in CD1d molecules among primates. Tissue Antigens 66:674–682
24. Sasaki A, Kudoh S, Mori K, Takahashi N, Suzuki T (1997) Are BCG effects against urinary bladder carcinoma cell line T24 correlated with apoptosis in vitro? Urol Int 59:142–148
25. Takahashi H, Nakagawa Y, Leggatt GR, Ishida Y, Saito T, Yokomuro K, Berzofsky JA (1996) Inactivation of human immunodeficiency virus (HIV)–1 envelope-specific CD8+cytotoxic T lymphocytes by free antigenic peptide: a self-veto mechanism? J Exp Med 183:879–889
26. Takeuchi J, Watari E, Shinya E, Norose Y, Matsumoto M, Seya T, Sugita M, Kawana S, Takahashi H (2003) Down-regulation of toll-like receptor expression in monocyte-derived Langerhans cell-like cells: implications of low-responsiveness to bacterial components in the epidermal Langerhans cells. Biochem Biophys Res Commun 306:674–679
27. Thalmann GN, Sermier A, Rentsch C, Mohrle K, Cecchini MG, Studer UE (2000) Urinary interleukin-8 and 18 predict the response of superficial bladder cancer to intravesical therapy with bacillus Calmette-Guerin. J Urol 164:2129–2133
28. Wang H, Yang D, Xu W, Wang Y, Ruan Z, Zhao T, Han J, Wu Y (2008) Tumor-derived soluble MICs impair CD3(+)CD56(+) NKT-like cell cytotoxicity in cancer patients. Immunol Lett 120:65–71

JOURNAL OF VIROLOGY, June 2008, p. 6039–6044 Vol. 82, No. 12
0022-538X/08/$08.00+0 doi:10.1128/JVI.02753-07

Small Intestine CD4$^+$ T Cells Are Profoundly Depleted during Acute Simian-Human Immunodeficiency Virus Infection, Regardless of Viral Pathogenicity$^\nabla$

Yoshinori Fukazawa,[1]† Ariko Miyake,[1,2]† Kentaro Ibuki,[1] Katsuhisa Inaba,[1] Naoki Saito,[1] Makiko Motohara,[1] Reii Horiuchi,[1] Ai Himeno,[1] Kenta Matsuda,[1] Megumi Matsuyama,[1] Hidemi Takahashi,[3] Masanori Hayami,[1] Tatsuhiko Igarashi,[1] and Tomoyuki Miura[1]*

Laboratory of Primate Model, Experimental Research Center for Infectious Diseases, Institute for Virus Research, Kyoto University, 53 Shogoinkawaramachi, Sakyo-ku, Kyoto 606-8507, Japan[1]; Laboratory of Tumor Cell Biology, Department of Medical Genome Sciences, Graduate School of Frontier Sciences, The University of Tokyo, Tokyo 162-8640, Japan[2]; and Department of Microbiology and Immunology, Nippon Medical School, Tokyo 113-8602, Japan[3]

Received 27 December 2007/Accepted 27 March 2008

To analyze the relationship between acute virus-induced injury and the subsequent disease phenotype, we compared the virus replication and CD4$^+$ T-cell profiles for monkeys infected with isogenic highly pathogenic (KS661) and moderately pathogenic (#64) simian-human immunodeficiency viruses (SHIVs). Intrarectal infusion of SHIV-KS661 resulted in rapid, systemic, and massive virus replication, while SHIV-#64 replicated more slowly and reached lower titers. Whereas KS661 systemically depleted CD4$^+$ T cells, #64 caused significant CD4$^+$ T-cell depletion only in the small intestine. We conclude that SHIV, regardless of pathogenicity, can cause injury to the small intestine and leads to CD4$^+$ T-cell depletion in infected animals during acute infection.

The highly pathogenic simian-human immunodeficiency virus (SHIV) SHIV-C2/1-KS661 (KS661), which was derived from SHIV-89.6 (23), replicates to high titers and causes the irreversible depletion of the circulating CD4$^+$ T cells during the acute phase of intravenous infection, followed by AIDS-like disease within 1 year (23). We previously reported that KS661 massively replicates and depletes CD4$^+$ T cells in both peripheral and mucosal lymphoid tissues during the initial 4 weeks postinfection (16). On the other hand, the isogenic SHIV-#64 (#64), which was derived from SHIV-89.6P, is moderately pathogenic. The genomic sequences of the two SHIVs differ by only 0.16%, resulting in a total of six amino acid changes in the products of the *pol*, *env-gp41*, and *rev* genes. The intravenous inoculation of rhesus macaques with #64 induces plasma viral burdens comparable to those induced by KS661 during the acute phase of infection and causes a transient reduction of the circulating CD4$^+$ T lymphocytes (10). After the acute phase, the viral loads decline to undetectable levels and the populations of CD4$^+$ T cells recover to preinfection levels.

To clarify the relationship between acute viral replication kinetics and subsequent clinical courses for these isogenic SHIVs with distinct pathogenicities, we examined proviral DNA, infectious-virus-producing cells (IVPCs), and CD4$^+$ T-cell depletion in peripheral and mucosal lymphoid tissues of 17 infected (Table 1) and 7 uninfected adult rhesus macaques (*Macaca mulatta*). Both Chinese and Indian rhesus monkeys were randomly assigned to these groups. The monkeys were used in accordance with the institutional regulations approved by the Committee for Experimental Use of Nonhuman Primates of the Institute for Virus Research, Kyoto University, Kyoto, Japan. The animals were inoculated via intrarectal infusion as described previously (17). Following serial euthanasia, tissues were collected and analyzed up to 27 days postinfection (dpi) as described previously (16, 17).

Gross virus replication was assessed by measuring plasma viral loads by reverse transcriptase PCR (16). By 6 dpi, plasma viral RNA levels became detectable in all the KS661-infected macaques (Fig. 1A) and three of seven #64-infected macaques (animals MM372, MM391, and MM374) (Fig. 1B). Although the plasma viral loads of the two groups at 13 dpi, when the virus loads reached their initial peaks, were not significantly different ($P = 0.1673$), the average load (± the standard deviation) in KS661-infected monkeys ($9.3 \times 10^8 \pm 15.9 \times 10^8$ copies/ml) was about 10 times higher than that in #64-infected monkeys ($6.3 \times 10^7 \pm 11.6 \times 10^7$ copies/ml). These results suggest that KS661 spread faster and reached a somewhat higher titer than did #64 when the viruses were inoculated intrarectally.

Levels of peripheral blood CD4$^+$ T lymphocytes in all the KS661-infected monkeys decreased substantially within 4 weeks (Fig. 1C). On the other hand, the reductions in the levels of CD4$^+$ T cells varied among the #64-infected monkeys (Fig. 1D). For example, MM378 did not exhibit any appreciable changes, even though the plasma viral RNA load in this monkey reached 2.6×10^7 copies/ml by 21 dpi (Fig. 1 B and D).

* Corresponding author. Mailing address: Laboratory of Primate Model, Experimental Research Center for Infectious Diseases, Institute for Virus Research, Kyoto University, 53 Shogoinkawaramachi, Sakyo-ku, Kyoto 606-8507, Japan. Phone: 81-75-751-3984. Fax: 81-75-761-9335. E-mail: tmiura@virus.kyoto-u.ac.jp.

† These authors contributed equally to this work.

$^\nabla$ Published ahead of print on 9 April 2007.

TABLE 1. Experimental schedule for individual monkeys[a]

Virus (inoculum size)	Monkeys examined at:		
	6 dpi	13 dpi	27 dpi
KS661 (2×10^3 $TCID_{50}$)	MM300, MM309	MM313, MM334, MM392, MM393	MM308, MM310, MM394, MM395
#64 (2×10^5 $TCID_{50}$)	MM379, MM390	MM372, MM373*, MM391	MM374, MM378

[a] $TCID_{50}$, 50% tissue culture infective doses; *, MM373 received 2×10^3 $TCID_{50}$ of #64.

These data suggest that the decline in circulating $CD4^+$ T cells in KS661-infected animals was more severe and more reproducible than that in the #64-infected monkeys.

Another highly pathogenic SHIV, SHIV-DH12R, is known to cause systemic and synchronous replication events in animals following intravenous inoculation (6). To reveal the spread of virus in monkeys following intrarectal infection, we measured proviral DNA loads in a variety of tissues as described previously (16). KS661 proviral DNA was detected not only in samples from the rectums, the site of virus inoculation, but also in peripheral blood mononuclear cells and some lymph nodes (LN) at 6 dpi (Fig. 2A), suggesting that the virus was already spreading systemically. At 13 dpi, when the viral RNA loads in peripheral blood increased to the highest titers, proviral DNA levels in all of the tissues examined also increased, with levels in most monkeys exceeding 10^4 copies/μg of DNA. The levels of proviral DNA in all the tissues declined remarkably by 27 dpi. In contrast, #64 proviral DNA was detected only in the rectum of one (MM390) of the two monkeys examined at 6 dpi (Fig. 2A). At 13 dpi, the amount of proviral DNA in each tissue sample from #64-infected monkeys ($<10^4$ copies/μg of DNA) was considerably smaller than

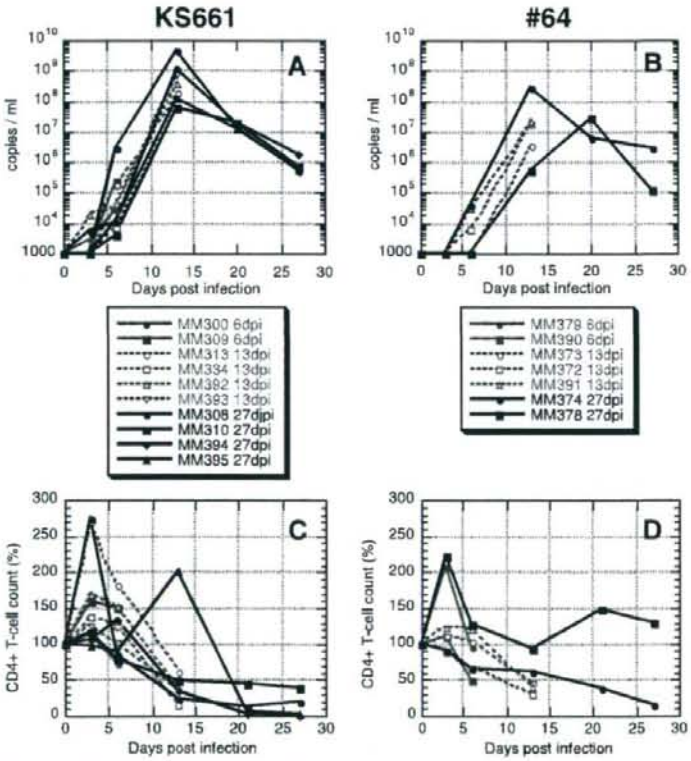

FIG. 1. Plasma viral RNA loads and profiles of circulating $CD4^+$ T cells for monkeys intrarectally infected with highly pathogenic KS661 and moderately pathogenic #64. (A and B) Plasma viral RNA loads were measured by quantitative reverse transcriptase PCR. The detection limit of this assay was 10^3 copies/ml. (C and D) Levels of $CD4^+$ T cells in peripheral blood samples from monkeys infected with KS661 and #64. The absolute number of $CD3^+$ $CD4^+$ cells in peripheral blood immediately before infection (day 0 postinfection) was defined as 100% for each monkey.